NOVA SCHOOL OF SCIENCE & TECHNOLOGY

DEPARTAMENT OF CHEMISTRY

António Francisco de Oliveira Gomes Barreira

BSc in Biotechnology

ALTERNATIVE FORMS OF LEVOTHYROXINE REPLACEMENT BASED ON FORMULATIONS WITH IMPROVED DRUG SOLUBILITY

MASTER IN BIOCHEMISTRY

NOVA University, Lisbon

March , 2023

DEPARTAMENT OF CHEMISTRY

ALTERNATIVE FORMS OF LEVOTHYROXINE REPLACEMENT BASED ON FORMULATIONS WITH IMPROVED DRUG

ANTÓNIO FRANCISCO DE OLIVEIRA GOMES BARREIRA

BSc in Biotechnology

Adviser: Doctor Márcia Ventura
Researcher, Chemistry Department, NOVA School of Science and Technology

Co-adviser: Professor Luís Branco
Assistant Professor, Chemistry Department, NOVA School of Science and Technology

Examination Committee:

Chair: Professor Sofia Rocha Pauleta

Rapporteurs: Professor Teresa Maria Alves Casimiro

Adviser: Doctor Márcia Ventura

MASTER IN BIOCHEMISTRY

NOVA University Lisbon
March 2023

Alternative forms of levothyroxine replacement based on formulations with improved drug solubility

ACKNOWLEDGMENTS

Agradeço em primeiro aos meus orientadores, Doutora Márcia Ventura e Professor Luís Branco por me terem aceite neste projeto, por me ajudarem também a enfrentar os desafios que fui encontrando ao longo do mestrado e principalmente por serem bastante flexíveis a nível de tempo e disponibilidade.

Quero desejar um agradecimento especial à Andreia Santos e à Doutora Clarinda Costa por me ter ajudado bastante neste projeto e ter tido imensa paciência.

Desejar também um agradecimento ao Zeljko Petrovski pela paciência e ajuda ao longo do mestrado

Quero deixar também um agradecimento às Professoras Ana Aguiar Ricardo, Madalena Dionísio e Ana Rita Duarte, por terem permitido a colaboração na execução de partes essenciais deste trabalho, à Doutora Rita Gameiro , pela realização dos ensaios de citotoxicidade e a Doutora Inês Paninho pela secagem dos aerogeis. Deixo também aqui um agradecimento a todo o pessoal do laboratório 517, 406 e 305, principalmente ao Afonso Bernardes. Gostava de agradecer também ao Dr. Nuno Costa (Laboratório de Análises do Departamento de Química) por todo o suporte (e paciência!) na determinação da levotiroxina por HPLC.

Aos meus amigos por me ajudarem, apoiarem e aliviarem dos nervos, foram muito importantes

Por último, mas não menos importantes agradecer às pessoas da minha vida que são a minha família por todo a ajuda e apoio durante este processo e também à minha namorada que foi muito importante nesta etapa.

Obrigado!

ABSTRACT

A substantial portion of the population is affected by thyroid diseases such as hypothyroidism. Levothyroxine is therapeutically used to treat hypothyroidism and to suppress thyroid stimulating hormone secretion in other thyroid diseases. In this work, three types of formulations were performed, starting with the synthesis of API-ILs based levothyroxine [T4] as a means to enhance [T4] solubility. For this matter [Na][T4] was combined choline [Ch] and 1-(2-hydroxyethyl)-3-methylimidazolium [C_2OHMIM] cations. These two prepared compounds and [Na][T4] drug were analyzed by proton and carbon NMR, ATR-FTIR, and elemental analysis. The serum, water and PBS solubilities of the API-ILs were compared to the [Na][T4] and for thermal analysis DSC studies were carried through. Permeability assays were performed, and an enhanced adsorption capacity was observed. Additionally, it was revealed by cytotoxicity assays that cellular viability in L929 cells was preserved. Having an higher solubility and a partition coefficient (K_d) slightly inferior to the one of levothyroxine sodium salt, the ionic levothyroxine formulation [T4][C_2OHMIM] can be considered as a potential alternative to levothyroxine commercial formulations with a good bioavailability. The second approach consisted on synthesis of aerogel matrixes based in a mixture two biopolymers kappa-carrageenan-locust bean gum (60%/40%) functionalized with ionic liquid [EOMIM][Br]. These biopolymers were characterized by SEM, ATR-FTIR, Nitrogen Adsorption-Desorption, DSC and TGA. A successful impregnation of the [Na][T4] drug and API-ILs synthesized into the aerogels with different ratios of functionalization (nf, 1:1, 1:6) was achieved. Finally, the third approach was the development of dry powder formulations, produced through Supercritical CO_2-assisted Spray Drying and subsequently assessed in Andersen-Cascade Impactor to evaluate aerodynamic properties. Furthermore, release assays with the dry powder's formulations were accomplished with [Na][T4]_DP presenting a faster release profile when compared to [Ch][T4]_DP.

Keywords: Sodium levothyroxine, API-ILS, bioavailability studies, biopolymers'aerogels, dry powders

RESUMO

Uma parte substancial da população é afetada por doenças da tiróide, tais como o hipotiroidismo. A levotiroxina é utilizada de forma terapêutica para tratar o hipotiroidismo e para suprimir a secreção hormonal estimulante da tiróide em outras doenças da tiróide. Neste trabalho, foram realizados três tipos de formulações, começando com a síntese de levotiroxina [T4] à base de API-ILs como meio para aumentar a solubilidade [T4]. Para esta parte a [Na][T4] foi combinada a colina [Ch] e os catiões 1-(2-hidroxietil)-3-metilimidazolium [C_2OHMIM]. Estes dois compostos preparados e o fármaco [Na][T4] foram analisados por RMN de protão e carbono, ATR-FTIR, e análise elementar. As solubilidades em soro, água e PBS dos API-ILs foram comparados com o [Na][T4] e para análise térmica foram realizados estudos de DSC. Foram realizados ensaios de permeabilidade e foi determinada uma capacidade de adsorção melhorada e adicionalmente, foi revelado por ensaios de citotoxicidade que a viabilidade celular em células L929 foi preservada. Tendo uma solubilidade superior e um coeficiente de partição (K_d) ligeiramente inferior ao do sal de levotiroxina sódio, a formulação iónica de levotiroxina [T4][C_2OHMIM] pode ser considerada como uma potencial alternativa às formulações comerciais de levotiroxina com uma boa biodisponibilidade. A segunda abordagem consistiu na síntese de matrizes de aerogel com base numa mistura de dois biopolímeros kappa-carragenano-goma de alfarroba (60%/40%) funcionalizados com líquido iónico [EOMIM][Br]. Estes biopolímeros foram caracterizados por SEM, ATR-FTIR, Adsorção-Desorção de Nitrogénio, DSC e TGA. A impregnação do fármaco [Na][T4] e dos API-ILs sintetizados nos aerogel com diferentes rácios de funcionalização (nf, 1:1, 1:6) foi bem sucedida. Finalmente, a terceira abordagem foi o desenvolvimento de formulações de pós secos, produzidos através da Supercritical CO2-assisted Spray Drying e subsequentemente avaliados no Andersen-Cascade Impactor para avaliar as propriedades aerodinâmicas. Além disso, os ensaios de libertação com as formulações de pó seco foram realizados com [Na][T4]_DP apresentando um perfil de libertação mais rápido quando comparado com [Ch][T4]_DP.

Palavras-chave: Levotiroxina de sódio, API-ILS, estudos de biodisponibilidade, aerogel de biopolímeros, pós secos

CONTENTS

LIST OF FIGURES

LIST OF TABLES

LIST OF ABREVIATIONS

API-ILs	Active pharmaceutical ingredient combined with ionic liquids
[Na][T4]	Sodium levothyroxine
[Ch][T4]	Choline levothyroxine
[C_2OHMIM][T4]	1-(2-hydroxyethyl)-3-methylimidazolium levothyroxine
ILs	Ionic liquids
K-C/LBG nf	Combination of kappa-carrageenan and locust bean gum (60%/40%) non functionalized
K-C/LBG 1:1	Combination of kappa-carrageenan and locust bean gum (60%/40%) functionalized with [EOMIM][Br] with a ratio 1:1 (m/m)
K-C/LBG 1:6	Mixture of kappa-carrageenan and locust bean gum (60%/40%) functionalized with [EOMIM][Br] with a ratio 1:6 (m/m)
FPF	Fine particle fraction
DP	Dry powder formulation
GSD	Geometric standard deviation
MMAD	Mass median aerodynamic diameter
NMR	Nuclear magnetic resonance

1

INTRODUCTION

1.1 Levothyroxine

Hormones from the thyroid are indispensable for normal growth and energy metabolism of most tissues in the body at all stages. Thyroid gland that is found in the neck is responsible for the production of thyroid hormones, when this gland does not process enough hormones for the requirement of the body, a clinical disorder take place named hypothyroidism. This condition is present in 5% of the population and an additional 5% is undiagnosed, meaning that this endocrine disorder is the second ordinary disorder following diabetes [1]. Hypothyroidism can be either congenital or being developed later in life. However, it is known that the majority of this disease rises with age and is higher in females than in males [2]. People with this condition may have different changes in their bodies, which can evolve into hypertension, cognitive impairment, dyslipidaemia, neuromuscular dysfunction and infertility [3]. This thyroid dysfunction is diagnosed bio-chemically, being the hypothyroidism described as serum thyroid-stimulating hormone (TSH) concentrations above and thyroxine concentrations below the normal reference range [4].

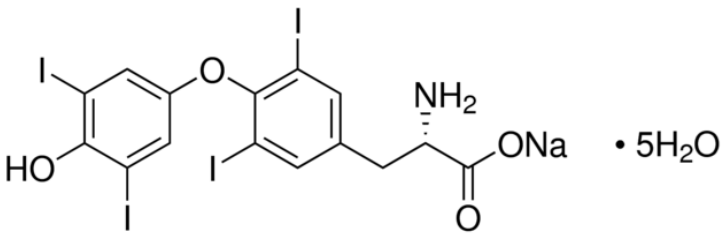

Figure 1 - Levothyroxine sodium salt pentahydrate

This condition can be treated, but not cured, the patients need to receive appropriate thyroid hormone replacement therapy and monitor their response. Most of the patients will

need a lifelong therapy taking synthetic [Na][T4] in form of oral administration as a means to alleviate the symptoms [5]. Considering a full replacement of thyroxine using levothyroxine, the addition of triiodothyronine in a low dosage can also provoke in some patients a mood or memory problems [6]. On top of that, for the patients who are unable to take the medication orally for an extended period, an alternative for that issue is an intravenous replacement. However, safe and functional alternatives to the oral administration of [Na][T4] should be pursued to avoid the parenteral alternative [7].

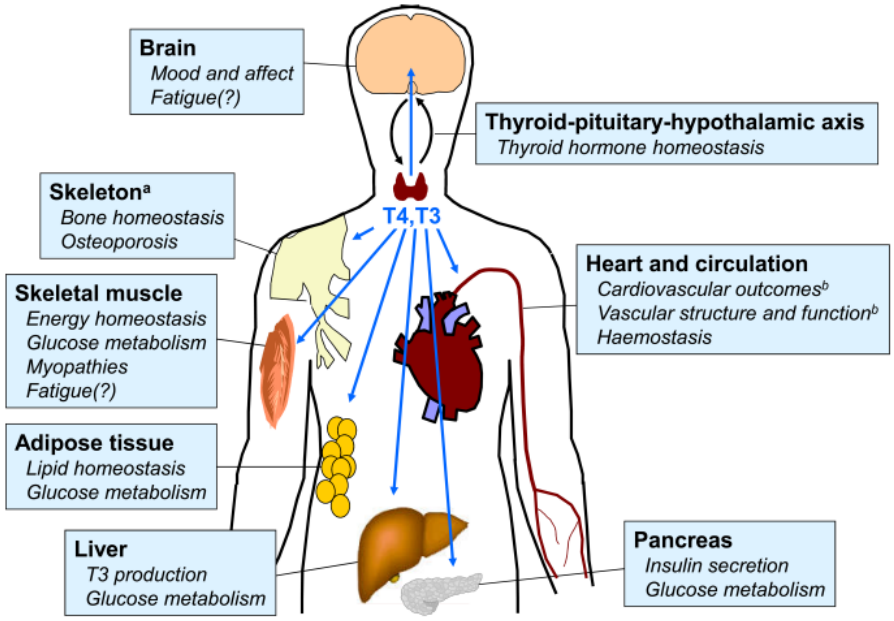

Figure 2 - Thyroid hormones principal targets. Subject of research (fatigue on the brain and skeletal muscle) marked with question marks [4]

Levothyroxine (T4) can be administered orally as sodium salt and its oral bioavailability is quite variable, ranging from 50 to 80% [8]. Formulations are available as oral solutions, capsules and tablets. The dosage in solid forms are formulated with the pentahydrate and the precision for drug administered to the patient is required and challenging due to its low dosage (25-300 µg/dose) [9]. It has been reported that 70% of novel medications exhibit low aqueous solubility, increasing the number of poorly soluble pharmaceutical drugs. The amount and speed of absorption and bioavailability of the drug are controlled by gastrointestinal permeability and the solubility of the drug [10].

1.2 Active Pharmaceutical Ingredients

Polymorphism is related to the capacity of solid matter to remain in 2 or more crystalline forms with different conformations or arrangements in the crystal lattice. This leads to different physicochemical properties like solubility, stability, dissolution, among others [11], [12]. Active pharmaceutical ingredients (APIs) are commercialized in crystalline arrangement, 40-70% of the drugs under development manifest a poor water solubility, which might jeopardize the therapeutic effectiveness and bioavailability and then originate a possible toxicity increase with side-effects [12], [13]. Bioavailability is an essential attribute of a pharmaceutical product, it quantifies the proportion of a drug which is absorbed and available to produce systemic effects [14]. The Biopharmaceutics Classification System (BCS) is a system that classifies bioavailability and so it characterizes drugs into four classes according to their US FDA permeability and solubility as illustrate in the figure 3 [15].

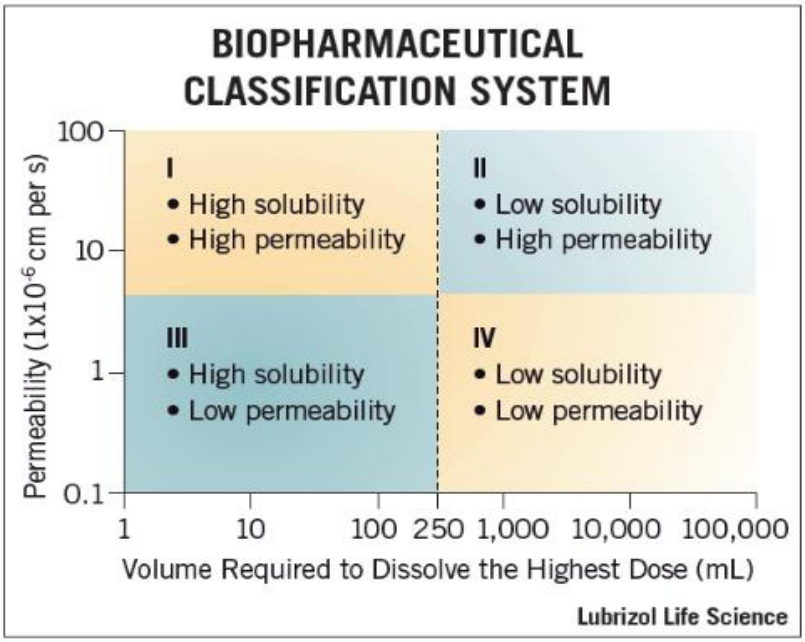

Figure 3 - Biopharmaceutical classification system [98]

1.2.1 Polymorphism and drug delivery

The production and the evolution of salts of specific active compounds is a worthy and conventional approach to solve polymorphism [16]. Nevertheless, co-crystals, polymer drugs and amorphous forms have been evaluated to subdue spontaneous polymorphic transformation of crystalline forms of drugs. These procedures can open on to consequential issues for pharmaceutical industries since it can turn an effective dose into a deadly dose by changing the solubility of the active ingredient [17].

Many reports of active drugs in cationic or anionic form combined with inert or biocompatible counter ions is increasing. A crucial step in preclinical stage of drug development is the creation and formulation of a desirable salt as a drug candidate, nowadays almost all pharmaceutical drugs used in medicine are administered as salts. The biopharmaceutical or physicochemical properties of a drug can be enhanced by combining a basic or acidic drug molecule with a counter ion to create a salt. The corresponding salts can provide diverse benefits over the original neutral formulations in terms of physical properties, such as crystallinity, melting point, hygroscopicity, dissolution rate and, in addition pharmaceutical properties, such as drug delivery, permeability, bioavailability. The salt forms of pharmaceuticals possess major effect on drug performance, safety and quality. Pharmacokinetics of a drug candidate can be seriously influenced by chosen counter ion, in particular its membrane transfer process or absorption. Salt formation is practically the only chemical method available to alter aqueous solubility and dissolution rate without altering the API. Other options for modifying these properties include the choice of polymorphic form, including solvents and co-crystal formation [17], [18].

1.3 Ionic liquids (ILs)

Ionic Liquids (ILs) are molten salts composed by an organic cation and an organic/inorganic anion, displaying unique features (e.g., higher thermal and chemical stability), being versatile regarding the chemical structure design [19]. An exponential growth in publications associated with the applications of ILs in pharmaceutical field is taking place, in last 20 years ILs have revealed a favourable ability to functionalize with biopolymers, opening avenues for their use as drug delivery systems [20].

Typically, they can be used for multiples purposes in organic chemistry, such as reaction mediators, extraction separation solvents and in electrochemistry as electrolytes. Moreover, the endless cation-anion combinations in ILs enable the use of pharmaceutical drugs as ionic components. Therefore, chloride and sodium are the most utilized, respectively as anions and cations for salt formation [20], [21] .

Active pharmaceutical Ingredient – Ionic Liquids (API-ILs) signifies that the API is in formation with ILs, this method lures a lot of attention because of it upgrades the drug stability, bioavailability and also the delivery in the biomedical field. In this area of study, ILs have proven an encouraging capability to functionalize iongels, aerogels opening a new direction for designing revolutionary materials for drug delivery systems. It has been reported to this day that API-ILs is used as an alternative to drug delivery involving mesoporous silica particles [22], [23]. A suitable selection of cations and anions will provide ILs an abundance of physicochemical properties, establishing an improvement by transforming or dissolving them into the IL. Choline cation is the most used in API-ILs [24][25], [26].

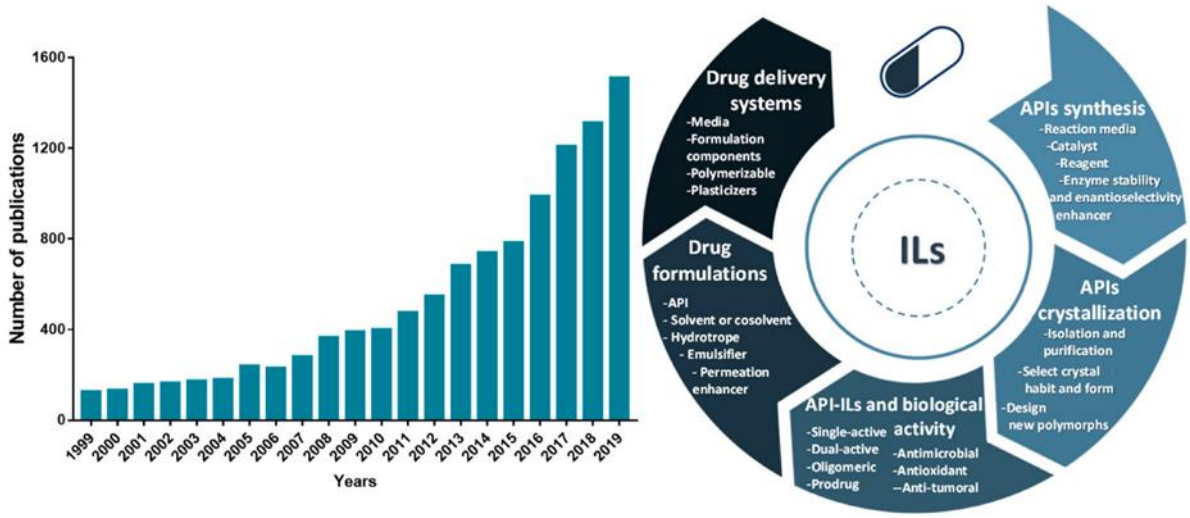

Figure 4 – 20 years of publications related to ILs and API [20]

Some interesting studies have been published using ionic liquids to improve water solubility of drugs like diclofenac, ibuprofen, ketoprofen, naproxen, sulfadiazine, sulfamethoxazole, and tolbutamide [27].

It has been proven that incorporating imidazolium, ammonium or pyridinium cations with ibuprofen as an anion promotes an higher solubility in biological fluids and water, as

well as a lower degree of polymorphism and systemic toxicity [28]. Another study using cholinium-based ionic liquids showed the improvement of naproxen water solubility up to 600-fold [29]. Moreover, the solubility of the drugs can also be enhanced by using the tetrabutylphosphonium cation combining to acidic APIs (diclofenac, ketoprofen, ibuprofen, sulfadiazine, naproxen, tolbutamide and sulfamethoxazole) into API-ILs [27], [30]. Ampicilin is also known as a drug associated to low water solubility, and consequently low bioavailability [31],[32].

Similar methodology (Ampicillin-based ILs) was performed using organic cations to improve bioavailability and it has been proven that ampicillin was enhanced regarding solubility in water [33]. Thus said, combining T4 with ILs may be an appealing solution to avoid polymorphism and improving their bioavailability, as well as dissolution rates and stability.

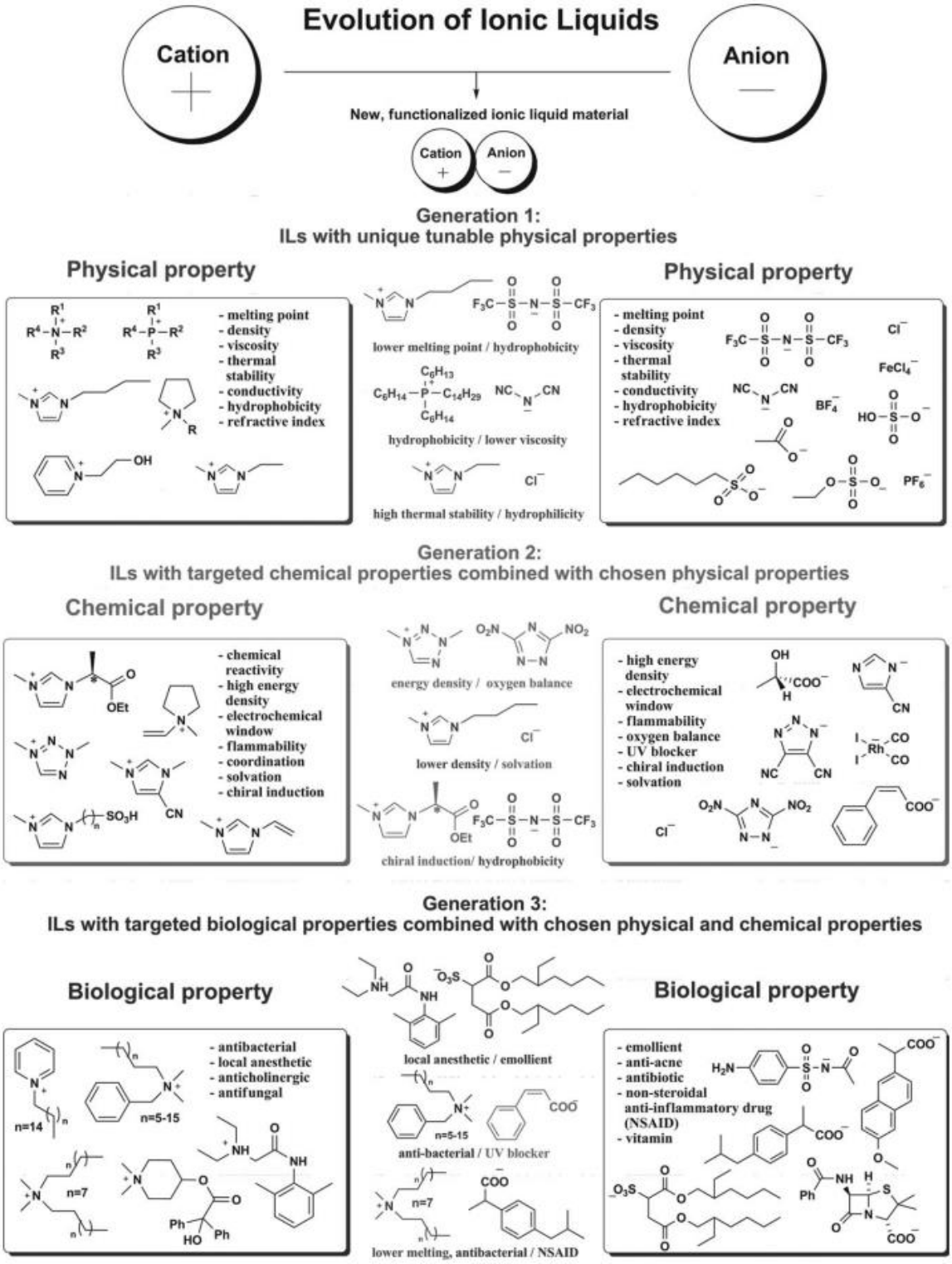

Figure 5 - Three generations of Ionic Liquids [34]

Ionic liquids have been known for over a century and a few years back being studied and analyzed worldwide to be used as solvents due to their unique physical properties (**Generation 1**) (Figure 5)

There is also a growing interest in enhancing physical and chemical properties of ILs for material applications (**Generation 2**) (Figure 5). Nowadays, the main objective is to obtain compounds with improved biological properties integrating APIs with ILs (API-ILS), in order to get the better of pharmaceutical issues (**Generation 3**) (Figure 5) [34].

1.3.1 Ionic liquids to avoid polymorphism

Surely the pharmaceutical industry faces many challenges, it has been difficult to emerge productive and sustainable new chemical entities and it is reported that scarcely any drugs that are evaluated make it to the market (<10%). Around 50% of the drugs are administrated as salts [35]. Properties of a drug can be modulated with many counterions, making it possible to adjust its properties with ionizable functional groups to get the better of unwanted characteristics present in the parent drug, parameters like melting temperature and solubility are fundamental because it influences the drug bioavailability and processing [36].

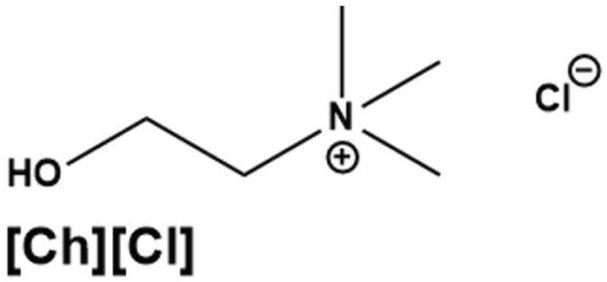

Figure 6 - Choline chloride structure

Pharmacokinetics of a selected drug can be influenced by the chosen ion pair as mentioned above, thus said, limitations encountered by pharmaceutical industry can be surpassed by the development of salts. Solid crystalline forms are used by drug companies due to the thermal stability, purity, facility of handling and manufacturability, although there are problems correlated with these forms, such as, low bioavailability, crystallization of amorphous forms and polymorphic conversion. For that reason, the use of liquid salts its appropriate, in preference to those with melting points below room temperature. The safety, quality, and performance of a pharmaceutical drug is linked to the salt structure [37].

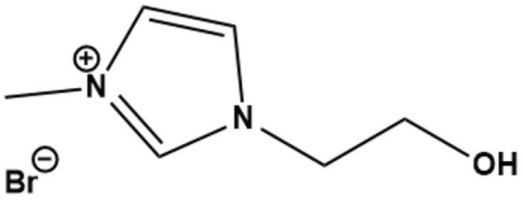

$[C_2OHMiM][Br]$

Figure 7 - 1-(2-hydroxyethyl) -3-methylimidazolium bromide structure

1.4 Improving API's bioavailability

1.4.1 Porous matrixes - Aerogels

Special class of nanoporous materials (aerogels) are gaining recognition and interest in biomedical and pharmaceutical applications [38]. The substitution of the liquid inside a gel with gas allows the transformation of an aerogel with the largest empty volume filled with air and other gases which contributes to the magnificent covering ability of aerogel materials. It also shows exceptional physical properties like ultralow thermal conductivities, extremely low densities and high specific surface areas and extraordinary capabilities for sorption of solvents, oil spills and metals as well as gases. Biopolymers aerogels are growing in the fields biomedical applications due to their mechanical properties sustainability, biodegradability and biocompatibility [39].

Supercritical process (Figure 8) to manufacture aerogels take into account the various changes of the liquid phase with organic solvents and after the extraction and drying under supercritical conditions. Liquid-solid adhesive forces and liquid-gas surface tension are avoided by this process, preventing the disintegration of the original pores. This method is compatible

withnmany solvents and enables the use of low water soluble materials. First aerogels produced were biopolymers'aerogels [40].

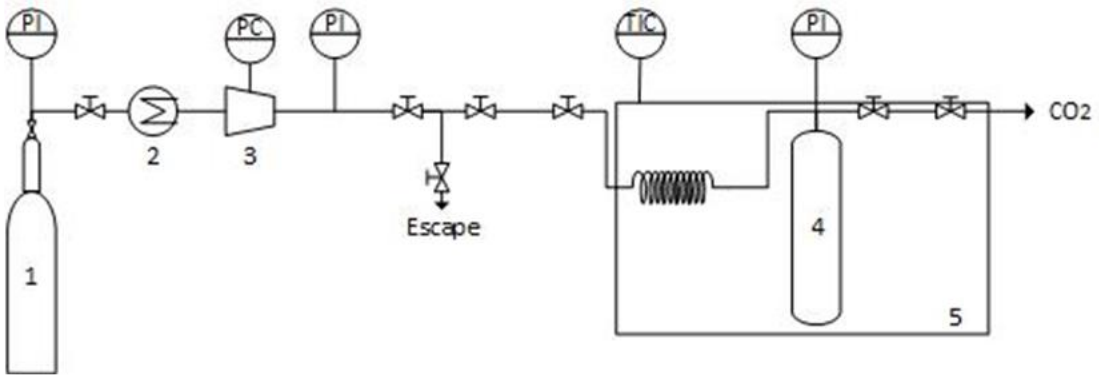

Figure 8 - Scheme of the supercritical drying facility; 1- CO2 tank; 2- Cooler; 3- Compressor; 4- Drying vessel; 5- Thermal bath; PI- Pressure Indicator; PC- Pressure Controller; TIC- Temperature Indicator and Controller [41]

1.4.2 Processing pathway

Process for the formation of an aerogel starts with development of a gel from an aqueous solution (hydrogel). The gels are formed by an induction of a cross-linking promoter that can be of chemical or physical nature into a solution. The succeeding procedure is to add a solvent, usually ethanol to substitute the water in the gel surface, leading to alcogels and finally, the ethanol extraction from the gel takes place by supercritical drying or free-drying. Biopolymers aerogels being biodegradable and biocompatible materials are beneficial and make them favourable carriers for drug delivery systems [38].

1.4.3 Natural polymers and biopolymers

Extracted polymers from animals and plants are considered promising ingredients and are playing an important role in the pharmaceutical industry, food industry and biomedical applications with the objective of replacing the synthetic polymers with the bio-inspired materials and to be used as adsorbents or carriers. Some characteristics that make polymers interesting are their ability to be biodegradable, economical, non-toxic, easy to acquire, and with few exceptions biocompatible. A Polymer created from natural sources, (bio)-chemically synthesized from a biological material and fully synthesized by microorganisms, and on top of that, being low cost and renewable is called a biopolymer. Unique properties such as non-

toxicity, biodegradability of biopolymers increase their applications such as in food, medical devices, and others. Different sources of biopolymers were explored for many years for pharmaceutical and biomedical applications. These investigations have given rise to a diversity of healthcare products that use biopolymers as an active ingredient [42].

1.4.3.1 Biopolymers in drug formulations and drug delivery

As a means to improve the treatment and therapy and also advance in the formulation of novel drugs delivery systems, the functionalization of the polymeric surface concede the ability to make these biopolymers unique when applicated for drug delivery. Carrageenan's are extracted from edible red seaweed belonging to the family of linear sulfated polysaccharides. These polysaccharides consist of chains of (1-3)-linked galactose and (1 → 4)-linked α-d-galactose, which are variously switched and reshaped to 3,6-anhydro derivatives depending on the extraction conditions and the source [43], [44].

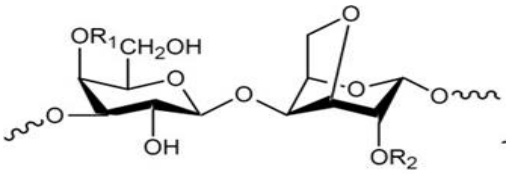

Figure 9 - Kappa-carrageenan structure
(Doi:10.1016/B978-0-12-801024-2.00005-4)

Three main types of carrageenans are recognized based on their patterns of sulfate-bound d-galactose units that are differently substituted and sulfate incorporated (kappa (κ), iota (ι) and lambda (λ) carrageenans) (Figure 9). Carrageenans tend to coil in higher concentrations around each other to form double helical structures due to their higher flexibility. A particular privilege is that they are thixotropic (time-dependent shear property). Because of their strong ionic nature, these biopolymers exhibit a high degree of protein reactivity. Some modified forms of carrageenans, which are used for drug delivery applications, are blended with carob gum, gellan gum and chitosan [45]. Locust bean gum comes from carob fruit, more specifically from the endosperm of the seeds, its white yellowish powder is obtain through crushing the pod present in carob fruit [46]. The structure of LBG features β-D-mannose units as the main chain, with 1→4 ether type bonds (Figure 10). The side groups consist of an α-D-galactose unit, which are linked to the main chain by 1→6 positions [47]. LBG is used to replace fat in many dairy products, is also being used to stabilize emulsions and dispersions and at relatively low concentrations LBG has the capability to originate very viscous solutions.

Moreover, this biopolymer usage in tissue engineering and drug delivery applications is increasing, it is adaptable with other gums such as carrageenan and act like a thickening agent to form a more elastic and stronger gel [48] [49].

LBG can also be used with other hydrocolloids such as carrageenans due to its synergetic action. K-C/LBG combinations are commonly used in several industrial food applications. When these two biopolymers are mixed depending on the preparation and production (temperature and weight ratio) it forms a network caused by the K-C and its rigidity caused by the LBG [50][51]. This synergetic interaction improves the properties of the films and edible films are formed by these interactions. It has been reported that this combination increases its tensile strength of the films compared to individually biopolymers films. The indicated improvement in gum films is reported due to the hydrogen bond interactions between K-C and LBG detected in FTIR analysis [52].

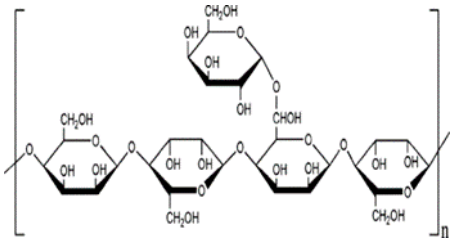

Figure 10 - Locust bean gum structure (Doi:10.1007/978-3-642-36566-9_5)

As mentioned above aerogels have been widely used in drug delivery, this form of formulation brings many advantages [53]. It has been investigated the drug loading and release for paracetamol and ibuprofen with two aerogels, alginate and starch. During this investigation the drug was loaded by adsorption directly into the aerogel from supercritical CO_2 and obtained good release profiles proving the physical properties like faster release from higher porosity materials [54]

Another example is the influence of biopolymers aerogels in the dissolution of low soluble drugs. The paper cited used pectin aerogels to study the release of nifedipine and it was concluded that the aerogel carriers significantly improved the dissolution and release of the drug [55]. These examples demonstrate the importance of the biopolymer aerogel approach to the drug release avoiding fracture and burst release of drug [56].

1.4.3.2 Functionalization of Biopolymers

Functionalized biopolymers are gaining popularity in industry, these macromolecules have chemical functional groups that differ from those of the backbone chains, for example, ionic functional groups on hydrophobic groups on polymer chains or hydrocarbon backbones. Biopolymer backbones are chosen due to their flexibility, mechanical strength, processability and chemical stability. This process of functionalization is based in chemical heterogeneity, improving reactivity, enhanced compatibility, and phase separation allowing to have extensive application in field of bioengineering [57].

Biopolymers combined with drugs by conjugation techniques have their own bioactivity enhancing the release kinetics and avoiding carrier accumulation in such a way that facilitates passive and active targeting, being then more beneficial than traditional small molecule therapeutics. This combination concedes the possibility for a drug to be released in a controlled deliver, offering a therapeutically effective dosage and also improves the drugs bioavailability (**55-65% of the drugs in creation have poor bioavailability**) [58].

1.4.3.2.1 Biopolymers functionalization with reactive ionic liquids

The functionalization of biopolymers can be done by the immobilization of reactive ionic liquids (ILs) through a transesterification reaction. The transesterification reaction begins by the activation of nucleophilic attack due to the protonation of C=O group by the acidic protons. After that the C=O group go through the nucleophilic attack by an OH group of a molecule from the biopolymer. Afterwards, proton relocation occurs. The charge shifts from the -OH group to $-O^+$ provoking the removal of the ethanol molecule. Ultimately, deprotonation of the resulting molecule take place and the final product of this reaction is obtained. An example of this reaction between [EOMIM][Br] and cellulose derivate is given in (Figure 11) [59].

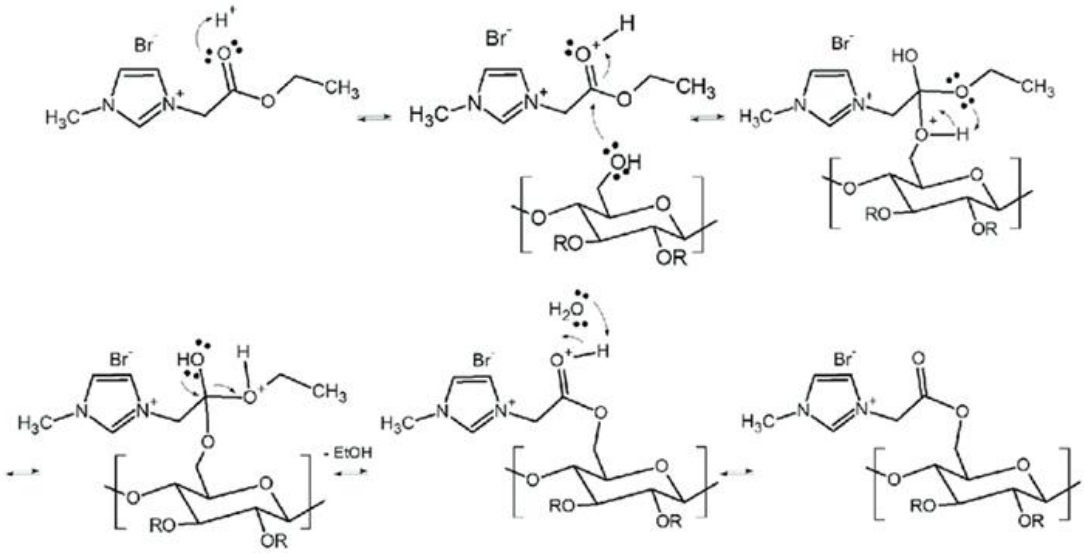

Figure 11 - Transesterification reaction between cellulose and [EOMIM][Br] [59]

1.5 Dry powder formulations

A non-invasive method of drug administration is a pulmonary drug delivery, it provides several advantages comparing to other administration routes, including an absence of extreme pH values, high vascularization for a rapid absorption into blood circulation, thin (0.1–0.2 mm) physical barriers for absorption and sizeable surface area (100 m^2). Additionally, this avoid of first pass metabolism leading to an higher bioavailability, less metabolic activity when compared to other locations of the body and a rapid systemic delivery from the alveolar region to the lung [60].

Above mentioned, oral administration have some side effects making this route important because it provides a quick action with lower doses causing reduced side-effects because of the rich blood vascularization and an increased surface area [61], [62].

Enormous investment in recent years have been made in dry powders systems for the controlled delivery of therapeutic molecules to the lungs. This system offers various advantages for pulmonary delivery such as, solid state stability of the formulation, ease of administration and low cost. Spray drying a common technique to acquire dry powders by atomization of a liquid solution into droplets through a spray nozzle producing dry molecules [63], [64].

Supercritical CO_2 is attained by increasing the pressure and temperature until it reaches the critical point, it behaves as a lipophilic and as a nonpolar solvent narrowed by polarity. The use of co-solvents has been suggested as an alternative to increase the solubility of the compounds and the extraction selectivity allowing operation at a lower pressure. [65].

In Supercritical CO_2-assisted Spray Drying (SASD), supercritical CO_2 acts as a co-solute for casting solution, leading to an atomization of the mixture through a nozzle and the droplets are subdivided due to vaporization of the CO_2 caused by an abrupt change in pressure. This process is more efficient. It is known that SASD provides a green and sustainable process to manufacture exceptional dry powders [66]. In order to make dry powder formulations excipients are requires. Trehalose is a sugar composed of two glucose molecules with an high glass transition temperature of aprox. 106 ^{o}C. This sugar forms a glassy matrix acting as a stabilizer for the inhalation powders. Nevertheless, trehalose is frequently combined with other excipients improving the stability of biopharmaceuticals. This disaccharide is hygroscopic and cohesive, creating a limitation for the dispersion of the powder formulation. Leucine is a nonpolar aliphatic amino acid and it is generally used as an excipient with treahalose. The addition of L-leucine to spray-dried formulations of APIs often result in a better in vitro aerosolization performance. Up to this point, there are no reports using SASD as a process applied to levothyroxine [67].

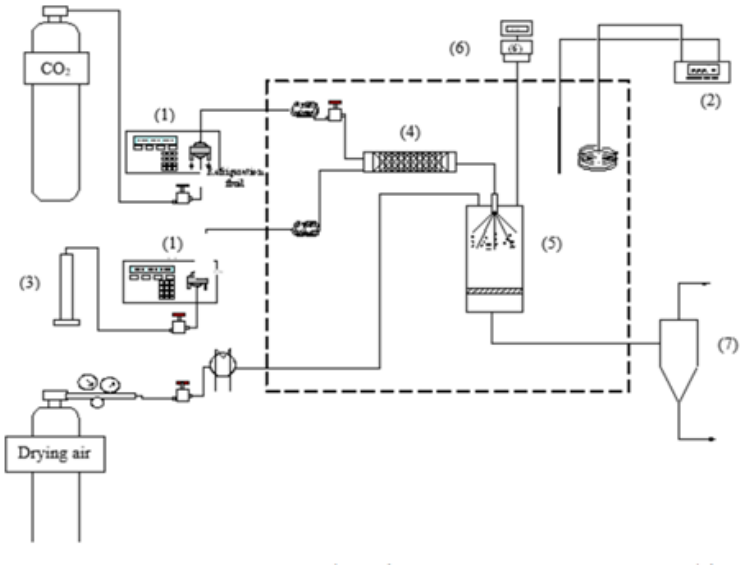

Figure 12 - Supercritical CO_2-assisted spray drying (SASD) (Doi:8. 788. 10.3390/pr8070788)

2

EXPERIMENTAL SECTION

2.1 Reagents and Equipment

The reagents listed below were purchased from different chemical suppliers.

Reagents acquired from Sigma-Aldrich:

- L-Thyroxine sodium salt pentahydrate (≥ 98%)
- L-Leucine (>98%)
- N-Methylimidazole (≥ 99%)
- Phosphate buffer pH 7.4
- Locust Bean Gum
- Dimethyl sulfoxide deuterated (>99%)

Reagents acquired from Cargil

- Kappa-carrageenan

Reagents acquired from Riedel-de Haen:

- Dimethyl sulfoxide (> 99%)

Reagents acquired from TCI:

- D-(+)-Trehalose Dihydrate (≥98%)

Reagents acquired from Alfa Aesar:

- Ethyl bromoacetate (≥ 98%)

Reagents acquired from Carlo Erba

- Chloroform (≥ 99%)

Reagents acquired from Fluka:

- Choline chloride Fluka (≥ 97%)

Reagents acquired from Air Liquide

- CO_2

Franz cells: PermeGear.de (ref: 4G-01-00-11.28-08)

Permeability membranes: Sartorius Stedium (ref: 15406-25-N)

For all synthesis, glass and plastic materials available from the laboratory were used. Equipments such as, analytical balance (Sartorious R200 D, Germany), rotary evaporator (Rotavapor R-100 BUCHI, Switzerland) and Schlenk line (Edwards RV5 vacuum pump, USA) were also used. NMR, FTIR-ATR, DSC, TGA and Porosimetry were performed in NOVA School of Science and Technology

Nuclear magnetic resonance (NMR) spectra were obtained via Bruker ARX400 400MHz at 298K, analyzed with MestreNova. The ^{1}H and ^{13}C spectra of all produced API-ILs with levothyroxine were acquired in deuterated dimethylsulfoxide (DMSO-d_6). Both deuterated solvents were acquired from Eurisotop.

Infrared spectra were executed on a PerkinElmer-two FTIR spectrometer equipped with a universal ATR sample accessory. The samples were studied in the 400 − 3700 cm^{-1} range.

Elemental Analyses (H, C and N) were conducted on an Elemental Analyser from Thermo Finnigan-CE Instruments Flash EA 1112 CHNS series (Analysis Laboratory of Chemistry Department—NOVA FCT, Lab. 211/213).

For the Differential scanning calorimetry (DSC), calorimetric analysis were accomplished on a DSC Q2000 from TA Instruments Inc. (Tzero DSC technology) coupled to RCS 90 cooling system and operating in the Heat Flow T4P option. For each experiment, 5−9 mg of sample were weighted and hermetically encapsulated in Tzero aluminium pans. Regarding the experimental procedure, all samples were previously equilibrated at 25°C and submitted further to different thermal treatments. For the samples with levothyroxine, several cooling and heating runs were performed to study the polymorphism addressed to the neat API.

The thermogravimetric analyses (TGA) were performed in a Thermogravimetric Analyser from Setaram Labsys EVO with weighing precision ±0.01 % from room temperature to 500 °C. The samples masses were between 8-10mg and each run was regulated at a heating rate of 5 °C min^{-1}, under a pure argon atmosphere purged at 50 mL min^{-1} (Analysis Laboratory of Chemistry Department—NOVA FCT, Lab. 211/213).

Scanning electron microscopy (SEM) was performed with a Hitachi S2400 microscope operating at 5 kV with a magnification x 20K. SEM micrographs were obtained by scanning electron microscopy. A gold film was settled onto the samples to minimize loading and improve image contrast. The SEM analysis were performed at IST-UL.

Nitrogen adsorption-desorption porosimetry: the textural properties of the K-C/LBG dried gels were determined by nitrogen adsorption isotherms obtained at 77 K. Degasification under vacuum (<1 mPa) at 60°C was applied to the samples before the measurements for at least for 12 h. Specific surface area was determined by the Brunauer-Emmett-Teller (BET) plots. The total pore volume was determined at a relative pressure (p/p_O) of 0.97. The t-plot method was applied for evaluation of microporosity. The average pore diameter and

mesoporous volume were estimated using the Berrett-Joyner- Halenda (BJH) method (Analysis Laboratory of Chemistry Department—NOVA FCT, Lab. 211/213).

HPLC analysis were obtained HPLC Agilent 1100, column Agilent Zorbax Eclipse XDB 5 micron 250 x 4.6 mm, eluition A - 0.01 M KH2PO4 pH 3 | B – Metanol, 0 minutes: 55%A; 10 min: 20%A; 15 min: 20%A; 20 min: 55%A; 25 min: 55%A, Qv = 0.7 mL/min, 28 °C, detection UV: 225 nm (Analysis Laboratory of Chemistry Department—NOVA FCT, Lab. 211/213).

X-Ray Diffraction was performed in a RIGAKU X-ray diffractometer (model Miniflex II) with automatic data acquisition (Peak search for Windows v. 6.0 Rigaku) using Cu K radiation (= 0.15406 nm) and working at 30 kV/15 mA. Diffraction patterns were collected in the range 2 = 2 − 55◦ with a 0.02◦ step size and an acquisition time of 1 min/step. These analysis were performed at IST-UL by Dr. Auguste Fernandes.

2.2 Methods

2.2.1 Synthesis of Choline Levothyroxine [Ch][T4]

Chloline chloride (14.9 mg, 0.14 mmol, 1.2 eq.) was dissolved in ethanol to a round-bottomed flask and then sodium levothyroxine (100 mg, 0,12 mmol, 1 eq) was slowly added. The reaction mixture was stirred at room temperature for 24h. Afterwards, the solution was filtered; the solvent was evaporated and dried under vacuum. The final product was obtained as hygroscopic pale-yellow solid (78,3 mg, 75%).

^{1}H NMR (400 MHz, $(CD_3)_2SO$) δ: 7.78 (s, 2H), 6.94 (s, 2H), 3.85 (m, 2H), 3.42-3.40 (m, 2H), 3.12 (s, 9H), 3.08 (m, 1H), 2.80-2.75 (m, 2H) ppm.

^{13}C NMR (400 MHz, $(CD_3)_2SO$) δ: 152.80, 143.93, 141.25, 125,17, 92.54, 88.60, 67.52, 67.49, 67.47, 55.64, 53.69, 53.65, 53.61 ppm.

FTIR-ATR: ν = 3398, 2921, 1603, 1538, 1380, 1223, 1180, 1082, 950, 900 cm $^{-1}$.

Elemental analysis calcd (%) for $C_{20}H_{24}N_2O_4I_4.9H_2O$ (1025.62 g.mol^{-1}): C 23.40, N 2.73, H 2.34; found: C 23.20, N 2.82, H 2.21.

2.2.2 Synthesis of 1-(2-hydroxyethyl)-3-methylimidazolium Levothyroxine [C_2OHMIM][T4]

1-(2-hydroxyethyl)-3-methylimidazolium bromide [68] (22 mg, 0.17 mmol, 1.5 eq.) was dissolved in ethanol to a round-bottomed flask and then sodium levothyroxine (100 mg, 0.12

mmol, 1 eq) was slowly added. The reaction mixture was stirred at room temperature for 24h. Then, the solution was filtered; the solvent was evaporated and dried under vacuum. The final product was obtained as hygroscopic pale-yellow solid (88 mg, 81%).

^{1}H NMR (400 MHz, $(CD_3)_2SO$) δ: 9.15 (s, 1H), 7.78 (s, 2H), 7.73(d, 2H, J= 12 Hz), 6.55 (s, 2H), 4.23 (t, 2, H, J=8Hz), 3.87 (s, 3H), 3.73 (t, 2H, J=8Hz), 2.78 (m, 1H), 2.80-2.75 (m, 2H) ppm.

^{13}C NMR (400 MHz, $(CD_3)_2SO$) δ: 153.03, 141.26, 137.45, 125,21, 123.77, 123.17, 92.53, 88.58, 59.84, 55.86, 52.07, 36.18 ppm.

FTIR-ATR: ν = 3398, 3146, 2851, 1614, 1536, 1398, 1240, 1162, 1053, 830 cm^{-1} .

Elemental analysis calcd (%) for $C_{21}H_{21}N_3O_5I_4.8H_2O$ (1046.62 $g.mol^{-1}$): C 24.00, N 4.00, H 2.00; found: C 23.97, N 3.59, H 2.16.

2.2.3 Solubility assays

The solubility assays were performed in water (25 ˚C/37 ˚C), phosphate buffer (37 ˚C), serum (37 ˚C) and ethanol (25 ˚C/37 ˚C) for the synthetized API-ILs and T4. Different temperatures were applied (37 ˚C and 25 ˚C). For the water and ethanol assays made at 25 ˚C the compounds were weighed in plastic flasks and with a micropipette a volume of 1mL was added multiple times until the homogenous solution was achieved. For the assays at 37 ˚C a water bath was prepared and the same procedure was performed.

2.2.4 Permeability assays

Permeability assays were carried out using a 8mL glass (PermeGear) Franz-type diffusion cell with an operative mass transfer area of 1 cm^2. Franz cells has two compartments, the one on the top is the donor compartment and it is loaded with 2mL of the samples dissolved in ethanol/water (25%/75%) with the concentrations of 50mg/L. The compartment below is the receptor filled with 8mL of ethanol/water (25%/75%). In the middle of the both compartments was placed a polyethersulphone (PES-U) membrane with 150 micrometers thickness and 0.45 micrometers pore size (Sartorius Stedim Biotech, Germany) and contained with stainless steel clamp. After temperature reached 37 ˚C the receptor compartment was stirred at 400 RPM using a magnetic bar and then aliquots of 400 microliters were removed from the receptor compartment at pre-established time periods (5 min and hourly from 1 to 8h) and fresh mixture of was added to complete the volume. The determination of the API diffused was performed by HPLC.

API-ILs permeability (P) through the membrane was determined based on equation:

$$-\ln\left(1-\frac{2Ct}{C0}\right)=\frac{2A}{V}\times P\times t \quad (1)$$

C_0 is the initial concentration in the donor compartment, C_t the concentration in the receptor compartment at time t, A is the effective mass transfer area, V is the total volume of solution in both compartments [69].

Diffusion coefficient (D) was determined based on the equation 2:

$$D=\frac{V1\times V2}{V1+V2}\times\frac{h}{A}\times\frac{1}{t}\ln\left(\frac{Cf-Ci}{Cf-Ct}\right) \quad (2)$$

where Ci and Cf are the initial and final concentration in the receptor compartment and Ct is the concentration in the receptor compartment at time t. V_1 and V_2 are the volume in the donor and in the receptor compartment respectively and h is the thickness of the membrane.

To measure the solubility of the solute in the membrane, the partition coefficient (K_d) is determined by equation:

$$K_d=\frac{P\times h}{D} \quad (3)$$

2.2.5 Cytotoxicity assays

Stock solutions preparation:

Stock solutions of T4, [Ch][T4] and [C_2OHMIM][T4] were prepared in DMSO at 10 mg/mL.

Cell viability assay:

L929 cell line were used to study the biological effect of the compounds, these cells were acquired from DSMZ – German Collection of Microorganism and cell culture GmbH. Eagle's Minimum Essential Medium (MEM, with 1.5 g/L sodium bicarbonate, non-essential amino acids, L-glutamine and sodium pyruvate, Corning) was also used for the L929 cells to be placed in a culture medium with 10% fetal bovine serum (FBS, Corning) and 1% penicillin-streptomycin (Corning). Cells were cultured in a humidified incubator at 37 ^{o}C, with 5% CO_2.

Solutions of T4, [Ch][T4] and [C_2OHMIM][T4] at 50 and 75 ppm, from a 10 mg/mL DMSO stock solution, were prepared in MEM and incubated with the cells for 24 h, at 37 ^{o}C. Cells incubated with complete media only were used as the negative control. DMSO was used for the untreated cells group at a maximum permissible concentration of 1%.

CellTiter 96® Aqueous One Solution Cell Proliferation Assay (Promega), which is based on tetrazolium active component ((3-(4,5-dimethylthiazol-2-yl)-5-(3-carboxymethoxyphenyl)-2-(4-sulfophenyl)-2H-tetrazolium, MTS) was used as a means to evaluate the cell viability. Microplate reader (VICTOR Nivo TM, PerkinElmer, USA) at 490 nm was also used to measure the amount of formazan product, as the absorbance is directly proportional to the number of viable cells in culture. Cell viability was expressed as percentage of cells exposed to extracts vs control. Statistical analysis was performed using GraphPad Prism 7.00 software. Two-way ANOVA test was performed, as well, as Tukey's multiple comparison test. Statistical differences were considered if $p < 0.05$.

The cytotoxicity assays were performed by Dr. Rita Gameiro (des-solve group).

2.3 Formulations

2.3.1 Aerogels'synthesis

2.3.1.1 Ionic liquid [EOMIM][Br] synthesis

In this synthesis, 10mL of chloroform was first added to a 25mL flask, then 0.8mL of N-Methylemidazolium was added, and 1.1mL of ethyl bromoacetate was also carefully added. After addition, it was left to heat (60 °C) and stir for 24 hours. Eventually the chloroform was evaporated using a rotary evaporator under vacuum for 3.5 hours.

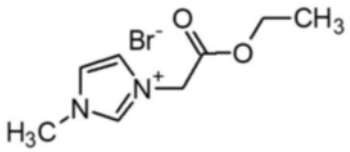

Figure 13 - IL [EOMIM][Br] structure

2.3.1.2 Functionalization of biopolymers with [EOMIM][Br]

In this preparation 25 mL of water was added into 50mL flask, a mixture of kappa-carrageenan and locust bean gum [K-C (60%)/LBG (40%)] with a total mass of 0.5 g was added with vigorous stirring for 60 minutes, at a temperature of 70 ◦C until the solution becomes transparent and without agglomerates. After the polymer dissolution, the [EOMIM][Br] was added and left to stir and reflux for 24 hours. Samples with different mass ratios of [EOMIM][Br] related to polymers, were prepared.

Samples:

- K-C/LBG nf - 100% K-C/LBG (31)
- K-C/LBG 1:1 - Equal amounts of polymer and IL [50% (m/m)]
- K-C/LBG 1:3 – 3x times excess of IL [150% (m/m)]
- K-C/LBG 1:6 – 6x times excess of IL [300% (m/m)]

After the 24 hours, the obtained mixture was introduced into cylindrical moulds to cool and solidify. After samples gelling the solvent inside the gel matrixes was changed by first adding 5 mL of an water/ethanol solution 50/50 (% v/v). The solvent exchange was performed for more 2 days by changing the composition of the water/ethanol mixture to 30/70 (%v/v) and 100 % ethanol. This step allows for a more effective elimination of the IL in excess which will be eventually inside the matrixes and constitutes a preparation for the sample drying step through supercritical extraction with CO_2, in order to obtain the aerogel.
The aerogels were characterized by SEM, N_2 - porosimetry, FTIR-ATR, DSC, TGA and elemental analysis.

2.3.1.3 CO_2 supercritical drying of the functionalized gels

Supercritical CO_2 drying of K-C/LBG produced matrixes was required for obtaining the aerogel. For this purpose, the supercritical CO_2 (Air Liquide) apparatus at NOVA's laboratory was used applying the following conditions:

- Pressure: 140 bar
- Temperature: 40 ˚C
- Time: 2 h

Supercritical drying of the aerogels was performed by Dr. Inês Paninho (CO_2 Conversion and Utilization group).

2.3.1.4 Drug loading into aerogels

Levothyroxine and the two produced API-ILs based levothyroxine compounds ([Ch][T4] and [C_2OHMIM][T4]) were loaded into the prepared aerogel matrixes. For this, solutions were prepared by dissolution of the compounds into DMSO assuring a levothyroxine concentration of 100 mg/mL. After, 3-5 mg of aerogel were placed in the glass vial containing compound solutions then left in controlled stirring at room temperature for about 24 hours in order to promote adsorption. After 24 hours the sample was removed and the excess DMSO was removed by washing the sample with fresh DMSO and then placed under vacuum at room temperature to be dried. The loaded compound mass was determined by gravimetry

and by HPLC after completely solubilizing/destroying the loaded sample in a determined volume of water (100mL). The load capacity q (mg of loaded compound per g of aerogel), of the different aerogels for the different synthesized samples was then determined.

2.3.2 Dry Powders

2.3.2.1 Particle Preparation

The solution was prepared by mixing Trehalose (2g) and L-Leucine (200mg) and Levothyroxine (8mg) with 80%(v/v) distilled water and 20% (v/v) ethanol. The particles were produced using the SASD apparatus. Briefly, liquefied CO_2 was pumped at 25 mL/min using an HPLC pump (Knauer HPLC pump K-501) and heated in an oil bath at 80 ^{o}C. In parallel, the casting solution was pumped at a rate of 3.5 mL/min, also using a high pressure pump (Knauer Smartline pump 1000). Both streams were delivered into the static mixer (3/16 model 37-03-075 Chemieer, 4.8 mm diameter, 191 mm length and 27 helical mixing elements), which was enrolled by a heating tape (85±5 ^{o}C), controlled by a Shinko FCS-13 ^{a} temperature controller. A near-equilibrium mixture was achieved by the CO_2 solubilization into the liquid solution in the static mixer. Then, it was atomized into a precipitator through a 150μm internal diameter nozzle. At the same time, a flow of heated compressed air (TAir=100 ^{o}C and FAir,in=30 m^3/h) entered the precipitator to evaporate the liquid solvent. The particles where then separated from the CO_2-solvent flow by a high-efficiency cyclone and collected in a glass vessel. The process's yield can be calculated as follows:

$$\eta\text{SASD}(\%) = \frac{\text{total mass after SASD (g)}}{\text{total mass before SASD (g)}} \times 100 \quad (4)$$

Dry powder API loading determines the percentage of API that composes the powder produced.

This parameter can be calculated as follows:

$$\text{API Loading}(\%) = \frac{\text{quantificated API mass (mg)}}{\text{total dry powder mass (mg)}} \times 100 \quad (5)$$

Dry powder API entrapment determines the percentage of API that composes the powder comparing the theoretical amount, taking yield into consideration. This parameter can be calculated as follows:

$$\text{API Entrapment}(\%) = \frac{\text{quantificated API mass (mg)}}{\text{theoretical API mass (mg)}} \times 100 \quad (6)$$

Dry powders preparation and ACI assays (see next chapter) were performed with the supervision of Dr. Clarinda Costa (Polymer Synthesis and Processing group).

2.3.2.2 Andersen cascade impactor assay

The evaluation of aerodynamic performance of the formulations was carried out using an aluminium Andersen Cascade Impactor apparatus (ACI, Copley). 30 mg of dry powder was loaded into three hydroxypropylmethylcellulose capsules nº3 (Aerovaus) and the capsules were individually placed into a previously weighed dry powder inhaler (DPI) that was coupled to the ACI device.

Individual plates of the cascade impactor were covered by a filter (Glass Microfiber filter MFV1080, Filter Lab) that is weighted before and after the experiment. The DPI punctured the capsule prior to the inhalation, and a high-capacity pump was used to simulate an intake of breath according to the European pharmacopoeia. After the intake, several aerodynamic parameters can be calculated from the amount deposited in each plate: fine particle fraction (FPF), mass median aerodynamic diameter (MMAD) and geometric standard deviation (GSD).

Firstly, MMAD gives the size of the particles that reached the impactor, except those deposited in the throat, representing the diameter of 50% the particles. Secondly, FPF determines the amount of the delivered particles sized below 5 µm, as determined by the interpolation of the percentage of the particles with smaller sizes than this value. Finally, the GSD measures the distribution of sizes of the particles, equation 7:

$$GSD = \frac{\sqrt{d84}}{\sqrt{d16}} \quad (7)$$

d8 and d16 are the diameters corresponding to 84 % and 16 % of the cumulative distribution, respectively.

2.3.2.3 Dry Powder release assay

For the release assay solutions of 50 ppm (%[Na][T4]) in PBS at 37 °C (pH 7,4) were prepared, dry powders formulations ([Na][T4]_DP and [Ch][T4]_DP) and sodium levothyroxine [Na][T4] were weighted as a means to attain the same concentration of the T4 in the all the solutions. The drug release assays were conducted in triplicate, 0,5 mL of the samples were taken out and the volume was restored with the same volume of fresh medium that was withdraw. Calibrations curves were obtained for a concentration of 1- 50 mg/L dissolved in ethanol/H_2O (%50/50) and the quantification of the drug formulations was achieved by HPLC. This experiment took place during seven days. The data for the drug dissolution was calculated with different mathematical kinetic models presented on Table 1.

Table 1 - Drug release curves acquired through adjusted mathematical kinetic models (Higuchi, Korsmeyer-Peppas, zero order and first order)

Kinetic Model	Equation (1)
Higuchi	$C=k_h t^{1/2}$
Korsmeyer-Peppas	$C=k_{kp} t^n$
Zero Order	$C=k_0 t$
First Order	$C=100\ (1-e^{k_1 t})$

In Table 1, the quantity of the drug released is defined as C for the instant t; k_0, k_1, k_h, K_{kp} represent release rate constants for the different kinetic models; n is the exponent of release (related to the drug release mechanism)in K-Peppas equation.

3

RESULTS AND DISCUSSION

3.1 API-ILs based levothyroxine

3.1.1 Synthesis of API-ILs based levothyroxine

The number of research publications on choline based ILs have been expanding showing its significance in many areas of research. Choline based ILs have been broadly used and applied in biological and pharmaceutical fields taking advantage of its non-toxicity and biodegradability [70]. In addition, several works focused on the synthesis and application of choline derivatives in different research areas including biotechnology.

Herein, levothyroxyne [T4] as anion was combined with two biocompatible cations based on choline [Ch] and 1-(2-hydroxyethyl)-3-methylimidazolium [C_2OHMIM] scaffold. The synthetic process was optimized using a simple anionic exchange by metathesis reaction starting from T4 sodium salt and correspondent halide cations. The desired T4-ILs salts, [Ch][T4] and [C_2OHMIM][T4] were purified in ethanol (by precipitation of the sodium chloride or bromide). The pure product was obtained in moderate to high yields (75%for [Ch][T4] and 81% for [C_2OHMIM][T4], respectively) and purity levels.

The elucidation of the chemical structure of each T4-ILs was performed by ^{1}H - ^{13}C-NMR (Appendix. 1 and 2), FTIR-ATR and elemental analysis. ^{1}H-NMR spectra allowed to proof the desired chemical structure of each salt as well as the cation-anion (1:1) proportion.

Figure 14 illustrates the ^{1}H-NMR of [Ch][T4] where all expected signals from cation and anion as well as respective integration was observed.

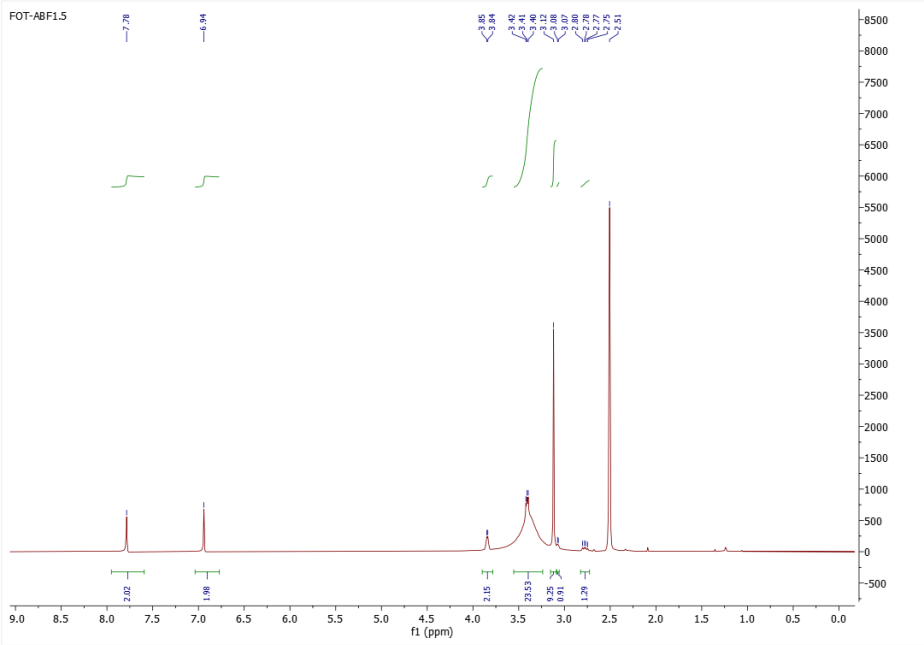

Figure 14 - ^{1}HNMR [Ch][T4] DMSO- d_6

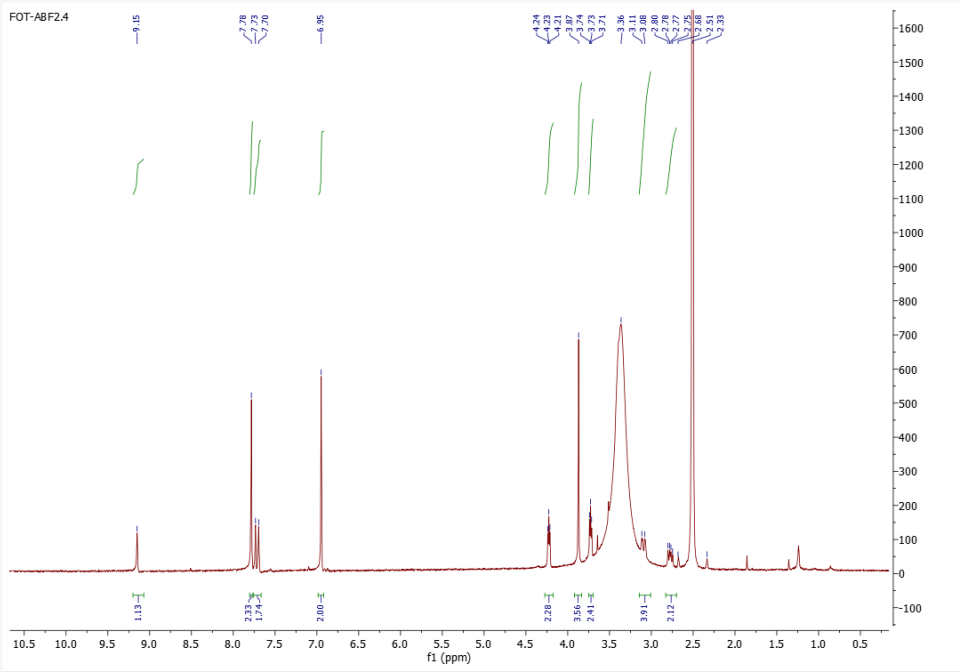

Figure 15 - 1HNMR [C_2OHMIM][T4] DMSO- d_6

Similar conclusions were achieved in the case of ^{1}H-NMR of the [C_2OHMIM][T4]. The confirmation of the expected structures were complemented by ^{13}C-NMR, FTIR-ATR and elemental analysis (H, C, N) for each prepared T4-ILs.

3.1.2 Characterization of the API-ILs by FTIR-ATR

Figure 16 illustrates the comparative FTIR-ATR spectra of original T4 sodium salt and each T4-ILs.

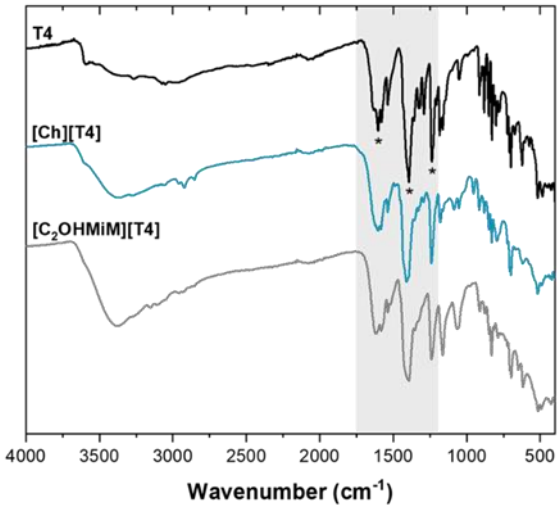

Figure 16 - API-ILs based levothyroxine FTIR spectra

The stretching vibration 3500-3450 cm^{-1} represents the crystallization water sustaining the pentahydrate form from T4. The 2940-2868 and 3043 cm^{-1} correspond to stretching vibration of the C-H from methylene group and aromatic rings. The band at 1620 cm^{-1} is the bending vibration of the latter bonds and others identified at 1420, 1500 and 1536 cm^{-1} represent the stretching vibration of the C=C bonds from aromatic systems. At 1560 and 1370 cm^{-1} the symmetric and asymmetric stretching vibration of C=O bond from the carboxylate anion are revealed and also it is possible to see at 1183 cm^{-1} the vibration of the C-O. The bending vibrations of the aromatic C-H are revealed at 1162, 920 and 878 cm^{-1}. Finally, C-N bond is observed at 1053 cm^{-1}. These results are according to the literature [71] [72]. Additionally, there is a peak between 900-980 cm^{-1} belonging to a specific group of quaternary ammonium compounds indicating the presence of choline cation. In addition, for IL [C_2OHMIM][Br] it is observed a band at 1600 cm^{-1} corresponding to the C=C stretching vibration and another for imidazolium ring at 1328 cm^{-1}.

3.1.3 Thermal Characterization

Since the knowledge of phase transformations and temperature resistance behavior of APIs is a crucial step when developing novel formulations, levothyroxine and both formulations were characterized by Thermogravimetric Analysis (TGA) until 500 °C and by Differential Scanning Calorimetry (DSC) between -90 and 150 °C. The respective thermograms are depicted in Figure 17, whereas the temperature values and enthalpies of the T4 thermal transformations are in Appendix.4. Moreover, the starting ionic liquids ([Ch][Cl] and [C_2OHMiM][Br]) were submitted to a similar DSC-procedure to evaluate their thermal events. Appendix.4 comprises the first and second temperature cycles of each halide organic salt.

Regarding the TGA results (Figure 16a), the weight loss curve found for neat T4 indicates

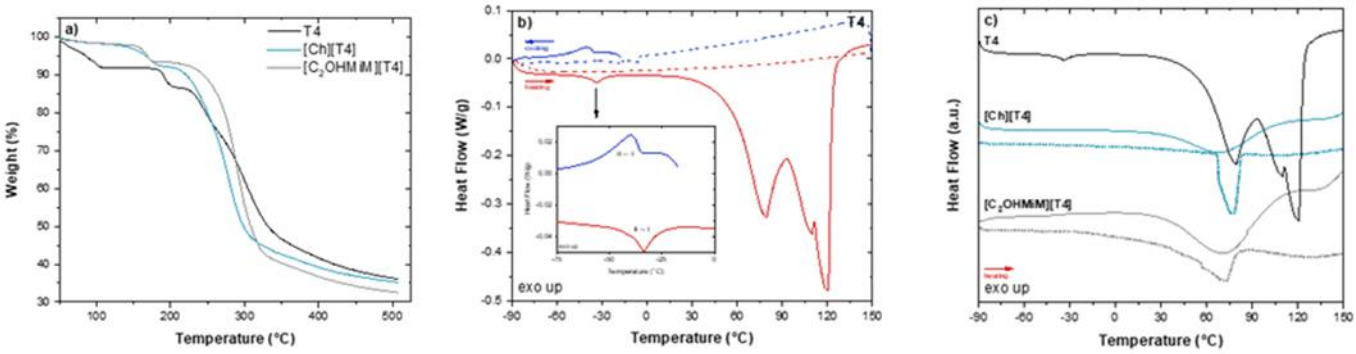

Figure 17 - Thermograms for a) the weight loss and heat flow trace of b) neat T4 and c) comparison between the first heating run of T4, [Ch][T4] and [C_2OHMiM][T4].

an ~10% weight reduction up to 100 °C, due to moisture loss from loosely bound adsorbed and coordinated water, in agreement with the thermal studies already published in literature [73] On the other hand, no significant weight loss was registered until 140−150 °C for [Ch][T4] and [C_2OHMiM][T4], which suggests that levothyroxine in both formulations loses the coordinated water. The respective ~2% mass reduction is associated to adsorbed water evaporation readily regained after the pre-drying treatment. Furthermore, for neat T4 the onset of the major decrease was detected at 175 °C, following a two steps degradation profile. A similar profile is detected for both formulations, although with an onset slightly shifted to lower temperatures: ΔT_{ons} ~50°C and ΔT_{ons} ~30°C, respectively for [Ch][T4] and [C_2OHMiM][T4].

The calorimetric analysis (Figures 17b and 17c) seems to confirm the dehydration behavior found by TGA: a multiple endotherm profile, attributed to the removal of adsorbed and coordinated water, is detected from ~35 to ~140 °C for neat T4. The registered thermogram is in accordance with previous studies [73] [74], however the temperature location is shifted due

to different water contents. A closer inspection of the cryogenic temperature range shows crystal-crystal transitions in T4 (-40 °C on cooling and -34 °C upon heating), coherent with polymorphism. In fact, it is already reported in literature that T4 can exist in distinct polymorphic forms [74][75]. It is worthwhile noting that the conversion between polymorphs is reversible proved by their detection in the first two cycles carried out up to 40 °C (see the inset of Figure 17b), a temperature insufficient to promote water evaporation. After heating up to 150 °C, water is successfully removed and no discontinuity in the heat flow curve is observed in the subsequent cooling and heating runs (dashed lines in Figure 17b). Moreover, if the commercial [T4] is vacuum dried prior to the calorimetric measurements no evidence of crystal-crystal transitions are detected.

The combination of levothyroxine with the two organic cations herein studied (Figure 17c) also leads to the disappearance of polymorphism, as only the broad endotherm assigned to water removal was detected in [Ch][T4] and [C_2OHMiM][T4]. After dehydration, no calorimetric response is registered for both formulations, as previously found for neat T4, indicating that the thermal behavior is dominated by the API, since the starting ionic liquids always display thermal events under thermal cycling. The DSC-traces of both formulations only exhibit the broad endotherm compatible with the elimination of freely adsorbed water.

Therefore, TGA and DSC studies allowed to conclude that both formulations promoted the loss of levothyroxine's coordinated water, also endorsing the disappearance of the polymorphism addressed to the T4. This is a relevant aspect in the context of pharmaceutical industry in which polymorphism could be a major drawback with a manifestation of unwanted effects [76].

3.1.4 Solubility assays

Levothyroxine is the centrepiece for hypothyroidism therapeutics, but its bioavailability can be restricted by many conditions, like interfering with medicaments and foods, concomitant diseases and noncompliance and that is why oral ingestion is the most suitable and commonly used route of drug delivery due to its ease administration. Many aspects influence the oral bioavailability like drug permeability, first-pass metabolism, dissolution rate, among others, being aqueous solubility the most frequent cause [77]. Sodium levothyroxine showed a tremendously low water solubility which is confirmed by the literature (0,150mg/mL, 25 °C, pH 7,4) [78] . In Table 2 are presented the obtained solubility data for [Na][T4], [Ch][T4] and [C_2OHMIM][T4] in different media and temperatures. For the synthesized API-ILs it is possible to observe an increase in solubility in water at 25 °C up to 2 times more than the original T4 and a significant increase (up to 3 to 4 times) is also observed in water at 37 °C. As mentioned above, both organic salts [Ch][Cl] and [C_2OHMIM][Br] have the ability to enhance low

drugs solubility. When levothyroxine is added to a phosphate buffer (PBS) solution its solubility is remarkably lower than in water. Evert, Henry E. reported that sodium levothyroxine solubility in PBS at 38 °C ranges between 2.5-5.0 ($\times 10^{-5}$) mol/L [79]. Thus said, solubility assays in PBS at 37 °C were performed with the [Na][T4], [Ch][T4] and [C_2OHMIM][T4] and the results once again turned our attention to the anionic exchange approach, it is possible to observe a boost in solubility up to 6 times by comparison with the one of original drug. Serum solubility assays at 37 °C were also performed and [Na][T4] showed slightly better results than the ones for the synthesized API-ILs.

Table 2 - Solubility (mg/mL) in water and PBS at 25 and 37 °C

Compound	**Water (37 °C)**	**Water (25 °C)**	**PBS (37 °C)**	**Serum (37 °C)**
[Na][T4]	0.149 ± 0.015 (1)	0.155 ± 0.002	0.163 ± 0.004 (1)	0.485 ± 0.005
[Ch][T4]	0.247 ± 0.035	0.386 ± 0.015	0.284 ± 0.017	0.334 ± 0.005
[C_2OHMIM][T4]	0.277 ± 0.034	0.379 ± 0.022	0.324 ± 0.004	0.321 ± 0.007

(1) Values for [Na][T4] solubility in PBS at 37ºC [79] and [Na][T4] solubility in water 25ºC [78]

3.1.5 Permeability assays

The permeability assays of [Na][T4], [Ch][T4] and [C_2OHMIM[T4] at 37 °C, pH 7.4 were performed for a maximum levothyroxine concentration of 50 mg L^{-1} in solution and up to 8 hours. Permeability and diffusion of the [Na][T4] can possible be changed when combined with ILs ([Ch][Cl], [C_2OHMIM[Br]) in aqueous medium. In this work we used a polyethersulphone (PES-U) membrane, distinct permeability and diffusion profiles were acquired. The diffusion coefficient is associated with the amount of API diffused with time, thus said, the increase of the diffusion coefficient is proportional to speed diffusion of the drug through a membrane. Another aspect is that solubility of the drug is proportional to the driving force. Regarding the results obtained for 8h permeability assay (Table 3), despite a higher solubility determined at 37 °C, the values determined for permeability and diffusion of the synthesized T4 salts are both lower than those determined for [Na][T4]. The greatest difference is observed for [Ch][T4] with a permeability value of 0.61 $cm.s^{-1}$ and diffusion of 0.10 $cm^2.s^{-1}$. For this salt, only 63% of the mass in the initial solution is identified in the receptor solution at the end of

the 8 h assay. The highest K_d value associated with [Ch][T4], 0.93, is indicative that the salt diffuses rapidly across the membrane but retention occurs to some extent.

Table 3 Diffusion (D), permeability (P) and partition coefficient (K_d) for the different studied compounds

Sample	Permeability (× 10^{-5}) cm/s	Diffusion (×10^{-6}) cm^2/s	K_d
[Na][T4]	2.04	0.49	0.63
[Ch][T4]	0.61	0.10	0.94
[C_2OHMIM][T4]	1.02	0.34	0.45

3.1.6 Cytotoxicity assays

Cytotoxicity assay was performed in L929 cells, commonly used for cytocompability studies. In Figure 18 it is presented the cell viability towards the L929 cells, after 24h exposure of T4, [Ch][T4] and [C_2OHMiM][T4] at 50 and 75 ppm. The presented data represent means ± SD (n = 3) and statistically significant differences were determined by Tukey's multiple comparisons test, two-way ANOVA.

It is worth noting that L929 cells can endure concentrations between 50 and 75 ppm without losing their viability. Additionally, these results suggested that the two concentrations of the T4-ILs herein explored do not impact the cytotoxicity. In fact, after 24 h of exposure to [Ch][T4] and [C_2OHMiM][T4], it is possible to assume that T4-ILs are non-toxic to the cells, as no significant differences between the test and the untreated control (DMSO) groups were found.

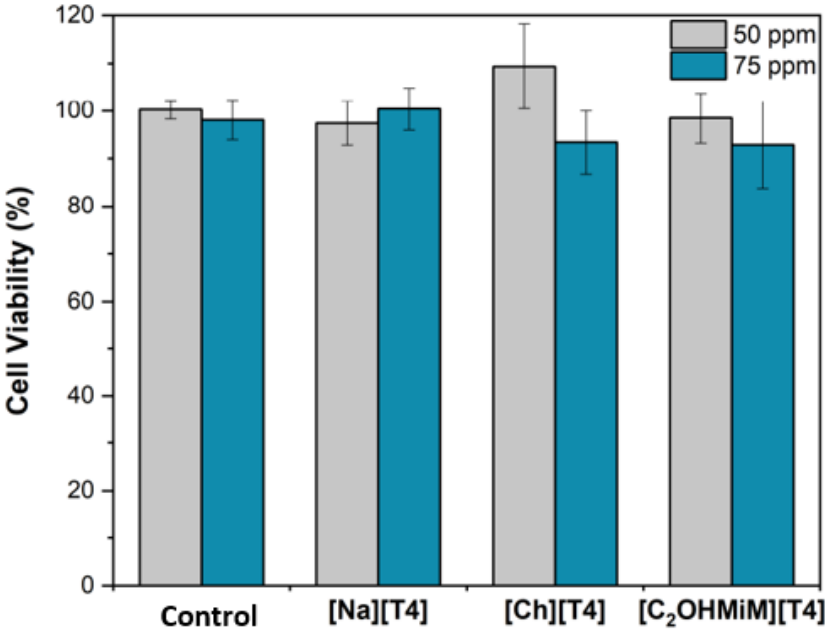

Figure 18 - Cell viability towards L929 cells after 24 h exposure to [Na][T4], [Ch][T4] and [C_2OHMiM][T4] at 50 and 75 ppm. DMSO was used for the control group at a maximum permissible concentration of 1%. Data illustrate the mean ± SD (n = 3), in which statistically significant differences, determined by Tukey's multiple comparisons test, are represented.

3.2 Biopolymers' Aerogels

3.2.1 Characterization of biopolymers' aerogels by FTIR-ATR

FTIR-ATR is a capable approach to explore biopolymers combinations. Changes are seen in FTIR spectra when chemical groups interact at molecular levels, for example, the shifting of absorption bands.

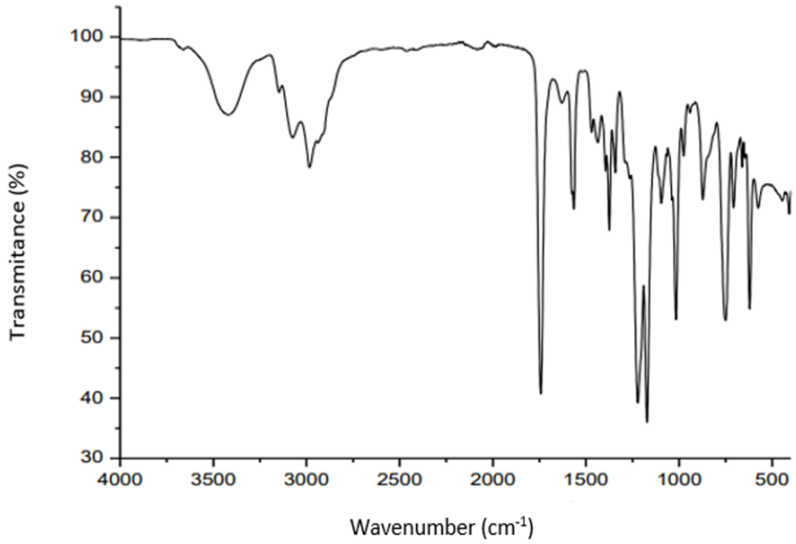

Figure 19 - FTIR spectrum of the IL [EOMIM][Br]

The FTIR-ATR spectrum of IL [EOMIM][Br] allows the visualization of the characteristic bands of the used ionic liquid. In the wavelength range between 2000-500 cm^{-1}, it can be observed the IL characteristic band at 1750 cm^{-1} that corresponds to stretching vibrations of the carbonyl C=O bond and the C–O stretches in the region 1300-1000 cm^{-1}. In the fingerprint region the imidazolium ring are observed bands at 1635 cm^{-1} and 1600 cm^{-1} that correspond to stretching vibrations of the C=C and C=N bonds, respectively.

Table 4 - FTIR bands attribution to the IL [EOMIM][Br]

Bands cm^{-1}	**Attributions IL [EOMIM][Br]**
3650-3200	O-H
3300-2700	C-H
1750	C=O
1635	C=C
1600	C=N
1241-1046	C=C

By analysing the FTIR spectra of the produced non functionalized sample (Figure 20), characteristic bands of both polymers and those resulting from their interaction can be identified. The bands observed between 1300-750 cm^{-1} are the ones corresponding to the carbohydrate's region.

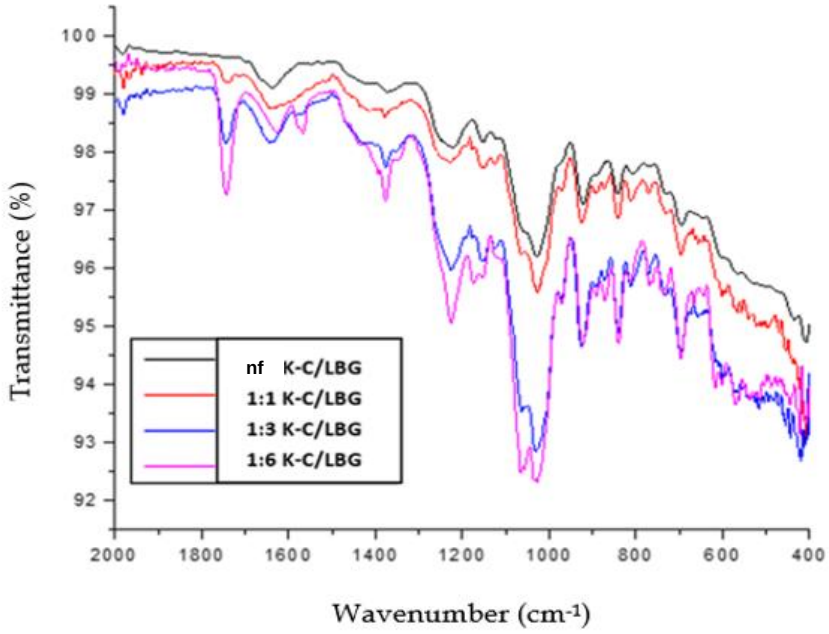

Figure 20 - FTIR spectra of the produced aerogel samples with different functionalization degrees

Sample functionalized with IL [EOMIM][Br] (K-C/LBG 1:3) ratio was prepared but not studied during this work since no significant differences from K-C/LBG 1:6 ratio were obtained.

The bands at 1175-1050 cm $^{-1}$ can be correlated to the interaction of the OH groups of LBG with K-C structure. The band at 936cm $^{-1}$ corresponds to C-O stretching, this peak at is related to the interactions between the two biopolymers through hydrogen bonding with unbranched smooth segments of the D-mannose backbone of LBG molecule. These results demonstrate physical entanglements and miscibility between K-C/LBG. These peaks go along with the ones reported on the literature [51].

Table 5 - FTIR bands of biopolymers K-C/LBG, nf, 1:1, 1:6)

Bands cm^{-1}	**Attributions K-C/LBGnf, 1:1, 1:6)**
3650-3200	O-H
3300-2700	C-H

1750	C=O
1600	C=N
936	C-O

In Figure 20, the spectra for the functionalized samples are also presented. By comparison with the one from non-functionalized sample, there are additional bands, that can be attributed to the presence of IL.

The intensity of these bands is higher for the higher ratios IL-polymer. The band at 1750 cm^{-1} corresponds to the carbonyl (C=O) bond on the IL [EOMIM][Br] and it can be observed that in the 1:6 ratio, this band has an higher intensity compared to the one from the 1:1 ratio sample, and also it is noticeable a slightly shift in 1:1 and 1:6 ratio (1758 cm^{-1} and 1763 cm^{-1}), respectively. The band at 1600 cm^{-1} related to the imidazolium rings on IL can also be observed for the samples with higher IL content. Bands between 1000 and 1300 cm^{-1} also intensify with higher concentration of IL for the three functionalized samples.

To support the FTIR results, by elemental analysis it is possible to quantify carbon, oxygen, hydrogen, nitrogen and sulfur atoms. From this information it is possible to estimate the possible functional groups that exist in biopolymers. Nitrogen is one of the elements that belongs to the IL [EOMIM][Br], from the in the Appendix.6 it is observed that the samples that contain IL [EOMIM][Br] K-C/LBG (1:1/1:6) have an higher percentage of nitrogen than the K-C/LBG which could indicate the presence of IL.

3.2.2 Textural Characterization

In Figure 21 are introduced the images of the prepared gels (left side) and the respective aerogels (right side). Non-functionalized and functionalized gels were soft and transparent

with diameters between 1-1.5 cm. There was no evidence for a significant volume shrinkage after the solvent exchange step and supercritical drying and the aerogels became stiff and white coloured. The SEM images obtained for the K-C/LBG aerogels with different degrees of functionalization are shown in Figure 21.

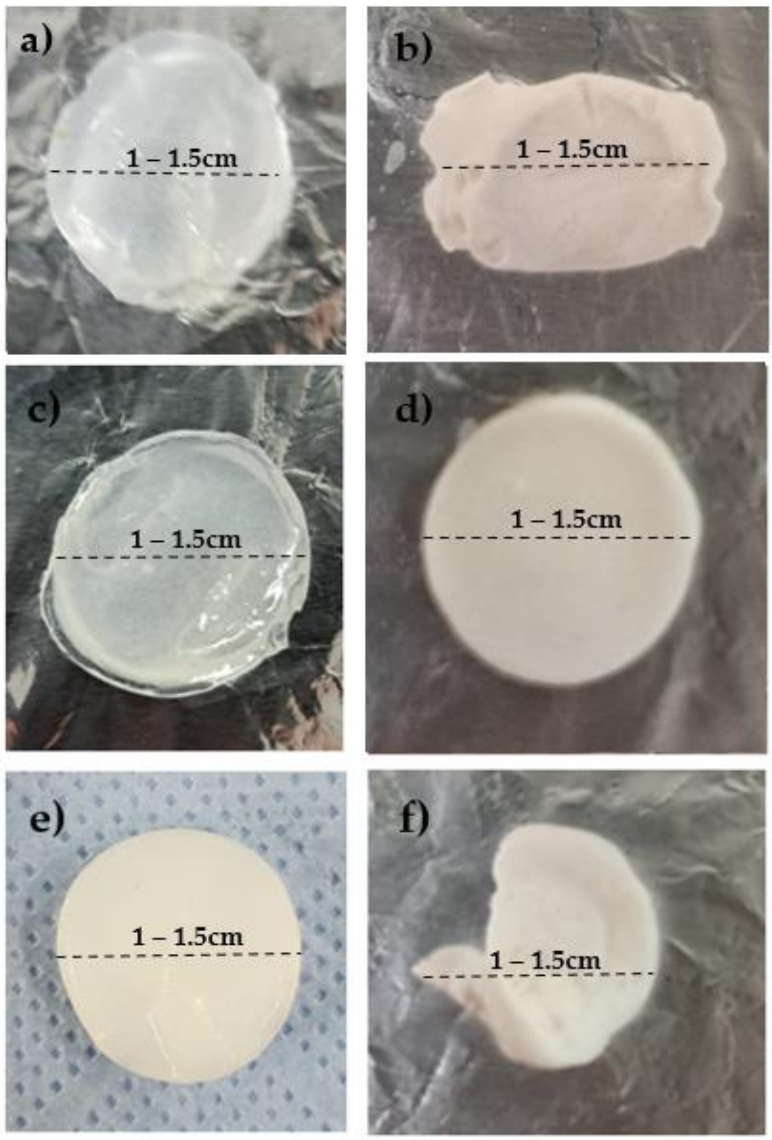

Figure 21 - Images of produced gels (left side) and aerogels (right side), a) K-C/LBG nf, b) K-C/LBG nf dried, c) K-C/LBG 1:1, d) K-C/LBG 1:1 dried, e) K-C/LBG 1:6, f) K-C/LBG 1:6 dried

3.2.2.1 Scanning electron microscopy (SEM) analysis

To evaluate samples surface SEM analysis was performed. The Figure 22 shows the images of K-C/LBG aerogels synthesized with different ratios in ionic liquid [EOMIM][Br] (K-C/LBG,1:1,1:6).

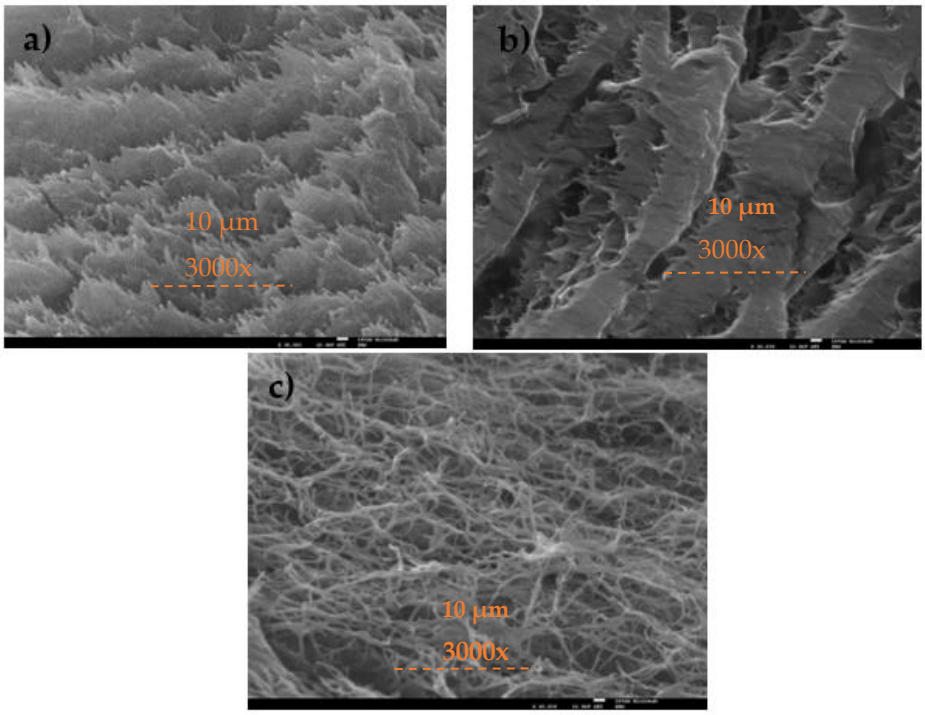

Figure 22 - SEM images of biopolymers non functionalized and functionalized with [EOMIM][Br: a) K-C/LBG nf, b) K-C/LBG 1:1, c) K-C/LBG 1:6

The Figure 22 image a), b) and shows the K-C/LBG non functionalized sample and K-C/LBG 1:1; 1:6 functionalized samples, respectively. By analysing the images it is possible to realize that the samples without the functionalization of IL [EOMIM][Br] (K-C/LBG nf) and with the functionalization 1:1 [50% (m/m)] exhibited a more dense fiber structure. However, a more visible interconnected fiber web structure containing a broad pore distribution including meso and mainly macropores is seen in the sample K-C/LBG 1:6 [(300% (m/m)]

3.2.2.2 Nitrogen adsorption-desorption porosimetry

The textural properties of produced K-C/LBG aerogels obtained by N2 adsorption-desorption porosimetry are presented in Table 6. The samples K-C /LBG nf and K-C/LBG 1:1 present similar values for the BET area and micropore volume, despite the lower value for total pore volume (meso and micropore volume) is presented for the K-C/LBG 1:1.

Table 6 - Textural properties of produced K-C/LBG aerogels

K-C/LBG dried gels	BET surface area ($m^2\ g^{-1}$)	Total pore volume ($cm^3\ g^{-1}$)	Micropore volume ($cm^3\ g^{-1}$)
[K-C/LBG] nf	201	0.95	0.03
[K-C/LBG] 1:1	243	0.53	0.02
[K-C/LBG] 1:6	59	0.11	< 0.01

The distribution for the micro and mesoporous for the two samples will have to be analyzed in order to justify the difference between the two BET areas. With a negligible microporous volume value and the smallest total pore volume value, the sample K-C/LBG 1:6 has a much lower BET area. These sample will be constituted mainly by porous with a macro dimension, fact that is supported by the obtained SEM images. Some of the values presented by the other authors: 320 $m^2\ g^{-1}$ for agar aerogels [80], 385 $m^2\ g^{-1}$ [81], 298-391 $m^2\ g^{-1}$ [82], 570 $m^2\ g^{-1}$, 390 $m^2\ g^{-1}$ [80], [83], [84], 150-300 $m^2\ g^{-1}$ [85] and 560 $m^2\ g^{-1}$ [80] for alginate aerogels and, 330 $m^2\ g^{-1}$, 150 $m^2\ g^{-1}$ [80], [83], [84], 472-750 $m^2\ g^{-1}$ and 845 $m^2\ g^{-1}$ [86] for chitosan and chitosan/silica composites. Ventura et al.[87] obtained BET values ranging from 60-180 $m^2\ g^{-1}$ for aerogels of locust bean gum. BET values obtained for produced gels even though they were lower, it is in range of values for polysaccharides aerogels comparing the produced K-C/LBG aerogels obtained with the presented by the authors.

3.2.3 Thermal characterization

3.2.3.1 Thermogravimetric analysis (TGA)

TGA was carried out to assess the thermal stability of the biopolymers functionalized with [EOMIM][Br], the thermogram is shown in figure 23.

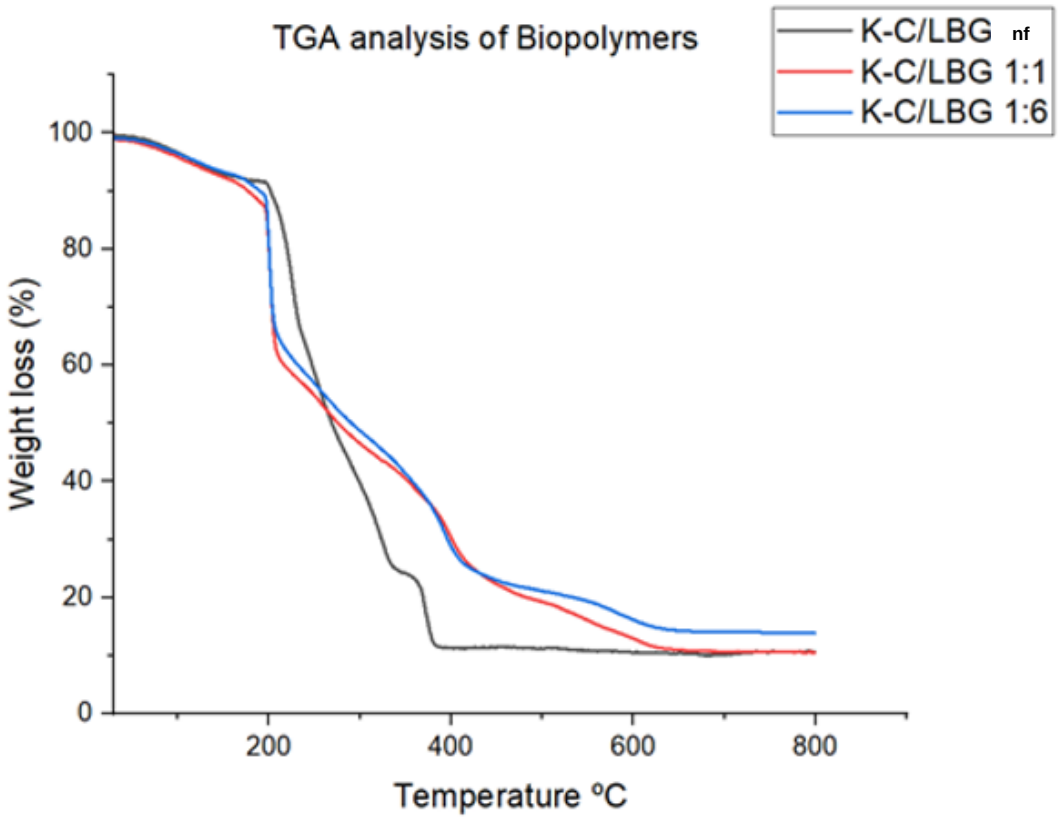

Figure 23 - Thermogram of functionalized biopolymers (K-C/LBG nf, K-C/LBG 1:1, K-C/LBG 1:6) with IL [EOMIM][Br]

Starting with the IL [EOMIM][Br] (Appendix 3), the first step starts at 39.16-188.51 °C and is related to the loss of water present in the ionic liquid, which occurs because [EOMIM][Br] easily absorbs water, this information is supported by FTIR spectra in figure 19, in which the presence of water is seen at peak 3650-3200 cm $^{-1}$. The step between 187.25-265.56 °C is related to the decomposition of imidazolium side chains (Appendix 7). For the thermal stability of K-C/LBG aerogels, the first step around 38-167°C corresponds to the water evaporation, second step is related to the fragmentation of biopolymer chains between 167-255 °C. The third step between 357-430 °C is correlated with the decomposition of the biopolymers, it is noticeable that in the third stage K-C/LBG exhibits less thermal stability compared with the

IL [EOMIM][Br] (Appendix 3) and the biopolymers functionalized (K-C/LBG 1:1; 1:6), this can be due to the interaction existing between the IL and the biopolymer by the transesterification reaction of ester groups indicating the presence of the IL in the biopolymers [59].

3.2.4 Drug encapsulation into aerogels

The amount of adsorbed compound was determined by gravimetry and by HPLC. The results for HPLC are presented in Table 7 and those for gravimetry on Appendix 6 in the annex. The characterizations by FTIR and DSC was performed as a means to support the results obtained (Table 7 Appendix 6). Unfortunately, neither FTIR or DSC was able to detect the drug impregnated in the aerogels (see Appendix 5; 9-13, respectively). The overall results obtained are consistent and show an higher adsorption capacity for the functionalized sample with lower IL's composition (K-C/LBG 1:1) and the non-functionalized sample (K-C/LBG). As it can be seen the sample K-C/LBG 1:6 had the worst outcome, fact that can be justified based on the characterization by SEM. In the referred sample, it is possible to observe pores with an higher dimension (essentially macropores) compared to the remaining aerogels, making it difficult to hold the drug inside the pore network. Since textural characterization is indicative that samples K-C/LBG, K-C/LBG 1:1 have similar pore and BET area features, it can be concluded that functionalization with [EOMIM][Br] might influence the sample´s drug absorption capacity. Taking into account the HPLC results (Table 7), the produced matrixes, present a lower adsorption capacity for [Ch]T4] than for the other two compounds. Apparently, the tertiary amine from [Ch][T4] is not interacting with the negatively charged sulphonated or carboxylic groups of the polymeric matrix, and/or is being repulsed by the positive charged amine from imidazolium group introduced on functionalization. Once [C_2OHMIM][T4] is adsorbed more easily, these interactions might be less relevant for the process of adsorption.

Table 7 - HPLC analysis of samples ([Na][T4], [Ch][T4], [C_2OHMIM][T4]) loading into aerogel

HPLC Analysis		
Loading with [Na][T4]	**mg of levothyroxine**	**q(1) (mg/g)**
K-C_LBG	6.5	1353.2
K-C_LBG 1:1	8.7	1673.1
K-C_LBG 1:6	6.1	1137.1
Loading with [Ch][T4]	**mg of levothyroxine**	**q(1) (mg/g)**
K-C_LBG	4.5	860.1
K-C_LBG 1:1	4.4	1146.8
K-C_LBG 1:6	2.2	393.4
Loading with [C_2OHMIM][T4]	**mg of levothyroxine**	**q(1) (mg/g)**
K-C_LBG	6.7	1431.5
K-C_LBG 1:1	8.2	1712.7
K-C_LBG 1:6	5.0	1501.5

(1) q is the loaded amount of drug per unit mass of aerogel sample.

3.3 Dry powders formulations

3.3.1 Characterization by FTIR-ATR of dry powders formulations

By examination of the FTIR spectra figure 24 it is possible to see the main peaks from [Na][T4] at 2950 cm $^{-1}$ and between 1700-1600 cm $^{-1}$ corresponding to amide band C-N and C=O, respectively. In addition, the peaks between 900-980 cm^{-1} and 950 cm $^{-1}$ belong to a specific group of quaternary ammonium compounds and C-N group of choline chloride, respectively. These peaks can also be seen in figure 16, indicating the presence of IL [Ch][Cl] in the dry powder's formulations.

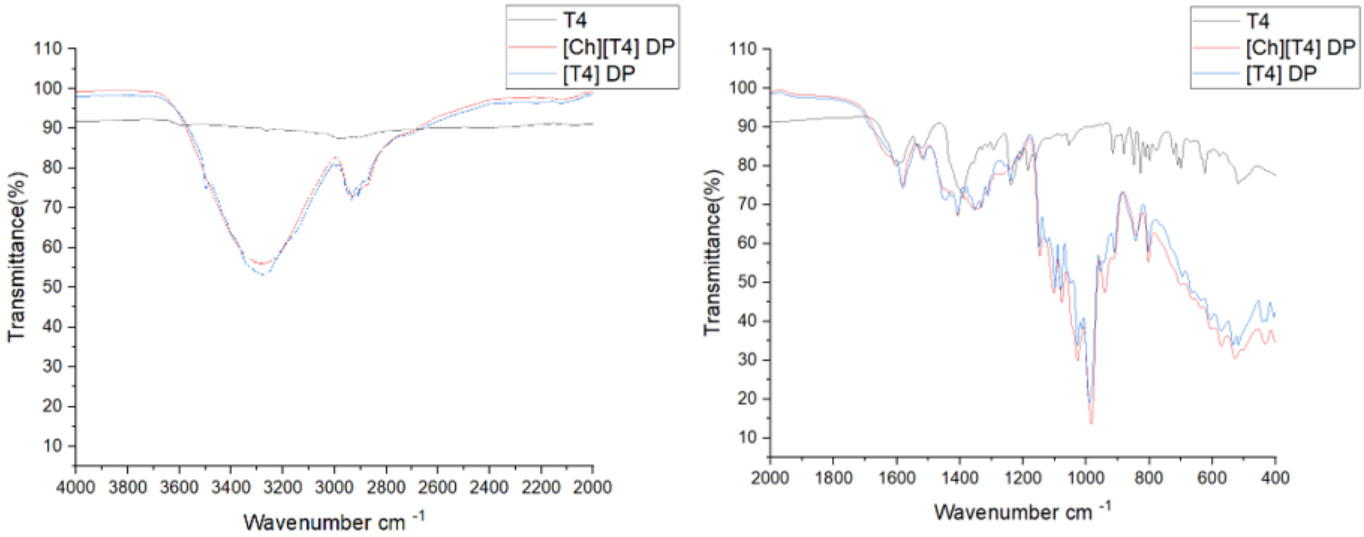

Figure 24 - FTIR spectra of dry powders formulations [T4], [Ch][T4] _DP and [T4] _DP

3.3.2 Scanning electron microscopy (SEM) Analysis

Morphology of the dry powders formulations was evaluated by SEM (Figure 25).

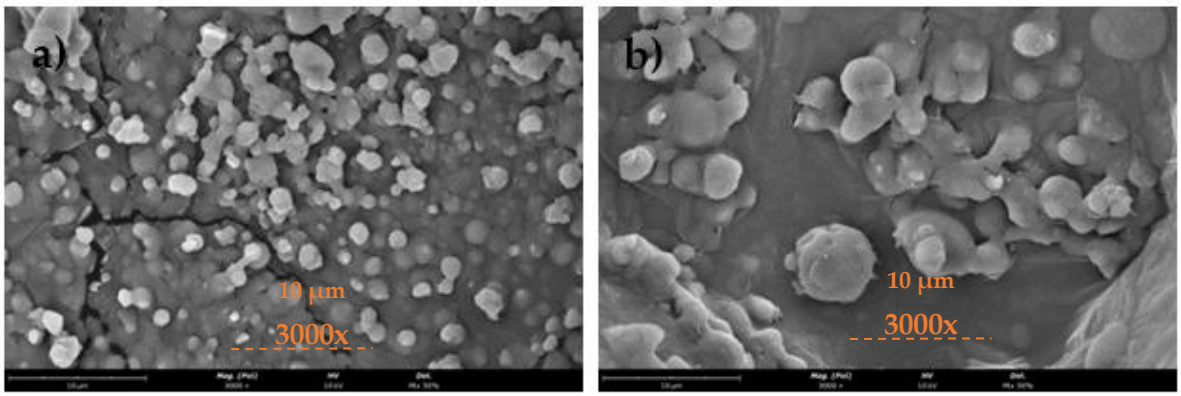

Figure 25 - SEM analysis of dry powders formulations ([Na][T4]_DP, [Ch][T4]_DP)

3.3.3 X-ray diffraction (XRD)

The results from X-ray diffractogram determines the crystallographic structure of a material. Figure 26 shows the X-ray diffraction patterns for [Na][T4], [Ch][Cl] and both formulations.

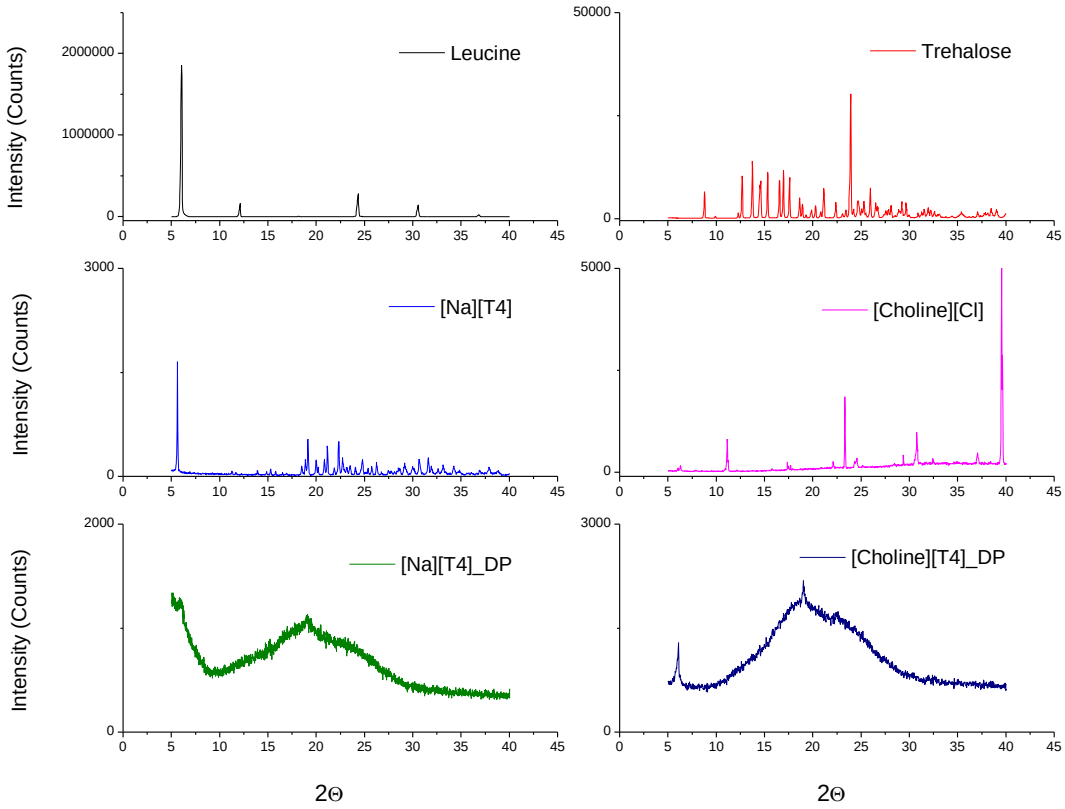

Figure 26 - X-ray diffractogram of dry powders formulations, leucine, trehalose, sodium levothyroxine and choline chloride

By analyzing the diffractogram it is possible to see that [Na][T4] presents a well-resolved x-ray diffraction patterns, this happens due to the fact that commercial sodium levothyroxine has a crystalline form and after a successful production of the dry powders formulations ([Na][T4]_ DP; [Ch][T4]_ DP), the crystalline form turns to an amorphous state as it is noticeable on account of the irregular x-ray diffraction pattern. Comparing both formulations the [Ch][T4]_ DP appears to be more crystalline than [Na][T4]_ DP, this fact is in agreement with the release assay (Figure 28) which indicates a lower release rate of the drug by the formulation [Ch][T4].

3.3.4 Production of [Na][T4] _DP and [Ch][T4] _DP

Levothyroxine sodium is prescribed for thyroid hormone replacement therapy, this drug is unstable, degrades rapidly and it is hygroscopic. Because of these limitations formulations of [Na][T4] have short shelf life. It is known that oral formulations are unable to deliver the drug into the blood at the same rate as injections, but on the contrary injections formulations can be painful for patients. In this work, successful development of dry powder formulations for both [Na][T4] and [Ch][T4] was achieved. These formulations might offer significant advantages over oral and other forms of drug administration, including enhanced bioavailability, improved dosage accuracy and safety, as well as accelerated absorption of the active pharmaceutical ingredient (API) into the bloodstream. Notably, there are no existing reports on the inhalation administration of [Na][T4]. The protocol for the production of sodium levothyroxine dry powders formulations ([Na][T4]_DP, [Ch][T4]_DP) composed of trehalose and leucine as excipient with levothyroxine as the API was adapted from Clarida et al. [88]. Due to the low solubility of levothyroxine in water the protocol had to be adapted to water/ethanol (80:20, % v/v). Using these experimental conditions an entrapment of 89.3% and 82.7% was achieved for the formulations [Na][T4]_DP and [Ch][T4], respectively and, a loading near 4% was obtained for both compounds in the produced formulations (see Table 8). The obtained dry powder formulations presented both a process yield near 60% which is a reasonable value considering that losses of powder can occur along the SASD system, being difficult to recover it.

Table 8 - Results from dry powders formulations production

Formulation	API	Solvent mixture	Loading %	Entrapment %	Yield %
[Na][T4]_DP	[Na][T4]	water/ethanol 80:20	4.30%	89.3%	58.70%
[Ch][T4]_DP	[Ch][T4]	water/ethanol 80:20	3.80%	82.7%	60.20%

3.3.5 Andersen Cascade Impactor (ACI)

Andersen Cascade Impactor stimulates a breath intake that leads the powder through a sequence of progressively smaller filters, it measures the flowability and aerodynamics of the powders.

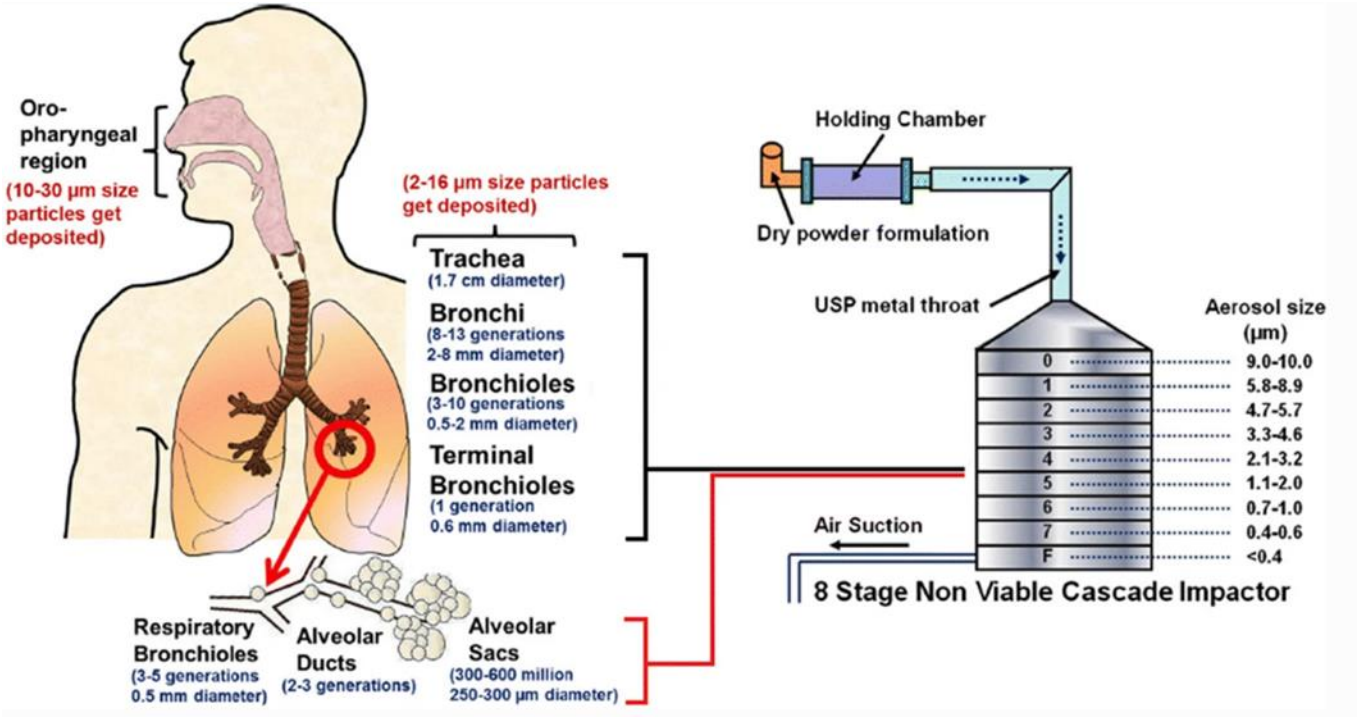

Figure 27 - Andersen-Cascade Impactor assay representation with lung dispersion correlation [100].

There's a correlation between the distribution of the powder through the stages (1-7) to how deep the powder would scatter through the lungs (Figure 27). The results obtained for both [Na][T4]_DP and [Ch][T4]_DP formulations were positive, as we can see from the table 9 the powders from [Ch][T4]_DP have MMAD values lower than [Na][T4]_DP, this indicates that the 50% of the particles obtained from the [Ch][T4]_DP assay can reach to the respiratory system, and also the FPF value is higher than [Na][T4]_DP, indicating that approximately 59% of the powder particles are less than 5 µm. Comparing both assays it is possible to conclude that [Ch][T4]_DP particles were finer with a better aerodynamics. This variation can be due to the more efficient drying process or to a more structured coating of the particles. In [89] a similar procedure was used to produce dry powders' formulations containing rifampicin The percentage value of FPF obtained for rifampicin was of 50%. Since there are no reports of inhalable dry powders of levothyroxine to this day and comparing these results with others reported in the literature using different pharmaceutical drugs, we can assume a positive outcome using this method [90].

Table 9 Results from ACI's experiments

Formulation	API	MMAD (μm)	FPF (%)	GSD
[Na][T4]_DP	[Na][T4]	1.996	56.453	2.193
[Ch][T4]_DP	[Ch][T4]	1.889	59.009	2.216

MMAD gives the size of the particles that reached the impactor,representing the diameter of 50% the particles. FPF determines the amount of the delivered particles sized below 5 μm. GSD measures the distribution of sizes of the particles.

Thus said the obtained API formulations reach the stage 5 terminal bronchi of the lungs, however the main objective was to reach the alveoli duct located in stage 6. Further assays need to be performed to improve these two formulations particle sizes and optimize its production protocol. Moreover, the drug loading achieved in the experiments was very low, therefore an improved drug loading must be accomplished to obtain a therapeutic loading of [Na][T4]_DP and [Ch][T4]_DP.

3.3.6 Dry powder release assay

The dissolution profiles of free [Na][T4] and, [Na][T4]_ DP and [Ch][T4]_ DP loaded into dry powders at physiologic pH 7.4 are shown in Figure 28.

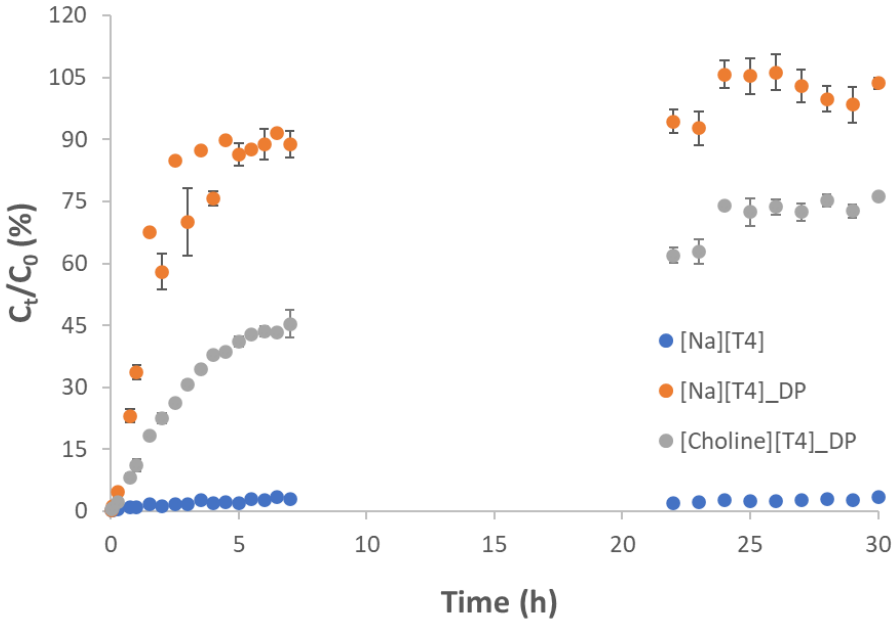

Figure 28 - Dissolution profiles for free [Na][T4] and, [Na][T4] and [Ch][T4] loaded into dry powders.

The assays were performed for a maximum levothyroxine concentration of 50 mg L^{-1} in solution and for no more than 2 days, once it was reported in the literature that the sodium levothyroxine is stable until 24h hours in phosphate buffer at 37°C [91].The dissolution of free levothyroxine was very low (C_t/C_0 < 0,02%), as expected, once the solubility into phosphate buffer for this drug at 37 ˚C is only 0.5 mg L^{-1}. The release plateau for [Na][T4]_DP was obtained close to the 24h with 100 % of the loaded drug released after this time. A plateau was also obtained for [Ch][T4]_DP near the 24 h but with a released amount near 76 %. Linear release (Table 10) is observed during the first 240 min, for both samples [Na][T4] and [Ch][T4], but the release is much faster for the first compound. From the DRX obtained for the prepared dry powders (Figure 26), it can be seen that [Na][T4]_DP present a more amorphous profile, with consequences on the solubility of the compound.

In Table 11 are represented the correlation factors (R^2) determined through the adjustment of the different kinetic models as presented in section 2.3.2.3 (Table 1), to the release curves.

Table 10 - The release rate values obtained for both studied cases considering the linear segment of release curve (zero order).

Samples	Linear release rate (% min^{-1})	Linear release (%)	Linear release time (min)	R^2	Final release (%)	Release time (h)
[Na][T4]_DP	0.371	75.7	240	0.841	103.6	24
[Ch][T4]_DP	0.162	37.7	240	0.989	76.3	30

Table 11 - Determination of Correlation factors (R^2) through the adjustment of different kinetic models

Samples	Higuchi	K.Peppas	Zero Order	First Order
[T4][Na]_DP	0.904	0.907	0.485	0.221
[Choline][T4]_DP	0.989	0.985	0.867	0.435

The two kinetic models K.Peppas and the Higuchi are the best fitted for both dry powders with a good correlation factor (R^2), however due to the swellable degree of both matrixes, it was considered that the K. Peppas kinetic model represents better the release mechanism of levothyroxine from dry powders. Table 12 exhibit the drug release determination the kinetic parameters through K. Peppas model, k_{kp} is the Korsmeyer release constant and n is an empirical parameter that characterizes the release mechanism.

Deducing that the samples have a spherical geometry it is possible to be assumed that the drug released in the referred compounds occurs by anomalous transport - diffusion along with swelling/matrix erosion – since n determined values are between 0.43 and 0.85 [92]–[97] . Thus said, the release mechanism is mainly controlled by diffusion for both samples, the fact that indicate this statement is that the determined value for kinetic parameter n are closed to 0.43 which indicates a pure diffusion mechanism on spherical geometry.

Table 12 - kinetic parameters determined for drug release through K.Peppas model

Sample	Model	Kinetic parameters
[Na][T4]_DP	K. Peppas	k_{kp} = 7.84 min^{-1}; n = 0.47
[Ch][T4]_DP	K. Peppas	k_{kp} = 2.88 min^{-1}; n = 0.49

4

CONCLUSION AND FUTURE PERSPECTIVES

In this experimental work, two API-ILS were synthesized by anionic exchange reaction using sodium levothyroxine (Na[T4]) and two halide salts from choline and 1-(2-hydroxy-ethyl)-3-methylimidazolium cations ([Ch][Cl]; [C_2OHMIM][Br]). Both desired API-ILs were successful prepared with yields between 78 to 81% and characterized by ^{1}H-NMR, ^{13}C-NMR, FTIR-ATR, elemental analysis, TGA and DSC to confirm its structure and thermal stability. It is possible to conclude that the two prepared API-ILs based on [T4] showed a drug transition from polymorph state to amorphous state. For the solubility assays API-ILs revealed a significant improvement (at least 2 times more) in water and phosphate buffer solubility at 25 and 37 °C comparing to commercial [Na][T4]. In the case of permeability assays, the diffusion profiles for API-ILs are higher comparing to commercial [Na][T4], although for the permeability profiles of [Na][T4] it exhibits better outcome compared to API-ILs, being significant higher than [Ch][T4] and slightly higher than [C_2OHMIM][T4]. The highest partition coefficient (Kd) was obtained for [Na][T4], which is the slightest soluble.

Cytotoxicity assays was performed in L929 cells and after 24h exposure of [Na][T4], [Ch][T4] and [C_2OHMiM][T4] at 50 and 75 ppm the cells can endure concentrations without losing their viability being possible to assume that API-ILS are non-toxic to the cells.

For the biopolymers'aerogels approach kappa-carrageenan (K-C) and locust bean gum (LBG) mixture (60%/40%) were successful prepared with different functionalization ratios (1:1, 1:3, 1:6) using the IL [EOMIM][Br]. FTIR, elemental analysis, DSC, TGA, SEM and porosimetry characterizations for the biopolymers'aerogels were performed. Thermogravimetric analysis (TGA) indicates that functionalized biopolymers K-C/LBG 1:1/1:6 exhibit higher thermal stability compared to K-C/LBG nf. Following porosimetry analysis the sample K-C/LBG 1:6 has much lower BET area compared to K-C/LBG/1:1 being constituted mainly by porous with a macro dimension, fact that is supported by the obtained SEM images.

Loading of [Na][T4] and both sinthesized API-ILS [Ch][T4] and [C_2OHMIM[T4] was carried out on the aerogels. The amount of loaded drug was evaluated by HPLC analysis. The sample [K-C/LBG 1:6] had the worst outcome because of the higher dimension of the pores making it difficult to hold the drug inside the pore network. The samples K-C/LBG and K-C/LBG 1:1, with similar textural properties, presented the best feature for the drug loading.

The produced matrixes, present a lower adsorption capacity for [Ch]T4] than for the other two compounds. Apparently, the tertiary amine from [Ch][T4] is not able to interact with the negatively charged functional groups of the polymeric matrix, and/or is repulsed by the positive charged amine from imidazolium group introduced on functionalization.

Alternative administration process was also achieved with supercritical CO_2 spray drying apparatus by producing dry powders using [Na][T4] and [Ch][T4]. Analysing X-ray diffractogram it is noticeable the amorphous state of the drug on the dry powders formulations ([Na][T4]_ DP; [Ch][T4]_ DP). By comparison of both samples, [Ch][T4]_ DP had better results than [Na][T4]_ DP, with 59% of FPF and MMAD of 1,89, making this approach very appealing for further studies. Furthermore, release assays were conducted for both formulations. Due to the more amorphous nature of the [Na][T4] sample, its release rate was found to be faster compared to [Ch][T4]. From these assays, it can be concluded that the drug release mechanism is primarily governed by diffusion in both samples.

For future work would be interesting to study release assay for impregnated biopolymers aerogels and evaluate the chemical stability for the new formulations produced.

BIBLIOGRAPHY

[1] L. Chiovato Flavia Magri Allan Carlé, "Hypothyroidism in Context: Where We've Been and Where We're Going," *Adv Ther*, doi: 10.6084/m9.figshare.9705650.

[2] O. Leng and S. Razvi, "Hypothyroidism in the older population," *Thyroid Research*, vol. 12, no. 1. BioMed Central Ltd., Feb. 08, 2019. doi: 10.1186/s13044-019-0063-3.

[3] B. Safaa, H. Al-Aazaui, and N. Q. Kadhim, "Role Of Anti-TPO And Some Other Biochemical Parameters In Serum Of Hypothyroidism Patients."

[4] G. J. Kahaly and U. Gottwald-Hostalek, "Use of levothyroxine in the management of hypothyroidism: A historical perspective," *Frontiers in Endocrinology*, vol. 13. Frontiers Media S.A., Nov. 02, 2022. doi: 10.3389/fendo.2022.1054983.

[5] M. I. Islam, M. Z. Ali, M. S. Islam, M. Solayman, and S. Hoque, "Hypothyroidism - A New View On An Old Disease," *KYAMC Journal*, vol. 7, no. 1, pp. 707–713, Aug. 2017, doi: 10.3329/kyamcj.v7i1.33764.

[6] Hueston WJ. Treatment of hypothyroidism. Am Fam Physician. 2001 Nov 15;64(10):1717-24. Erratum in: Am Fam Physician 2002 Jun 15;65(12):2438

[7] K. A. Obeidat, N. A. Saadeh, A. As'ad, and S. Bakkar, "Successful management of hypothyroidism in gastric outlet obstruction using levothyroxine rectal enemas: A case report," *American Journal of Case Reports*, vol. 19, pp. 903–905, Aug. 2018, doi: 10.12659/AJCR.909437.

[8] M. Tanguay, J. Girard, C. Scarsi, G. Mautone, and R. Larouche, "Pharmacokinetics and Comparative Bioavailability of a Levothyroxine Sodium Oral Solution and Soft Capsule," *Clin Pharmacol Drug Dev*, vol. 8, no. 4, pp. 521–528, May 2019, doi: 10.1002/cpdd.608.

[9] N. Kaur, V. G. Young, Y. Su, and R. Suryanarayanan, "Partial Dehydration of Levothyroxine Sodium Pentahydrate in a Drug Product Environment: Structural Insights into Stability," *Mol Pharm*, vol. 17, no. 10, pp. 3915–3929, Oct. 2020, doi: 10.1021/acs.molpharmaceut.0c00661.

[10] D. V. Bhalani, B. Nutan, A. Kumar, and A. K. Singh Chandel, "Bioavailability Enhancement Techniques for Poorly Aqueous Soluble Drugs and Therapeutics," *Biomedicines*, vol. 10, no. 9. MDPI, Sep. 01, 2022. doi: 10.3390/biomedicines10092055.

[11] R. Purohit and P. Venugopalan, "Polymorphism: An overview," *Resonance*, vol. 14, no. 9, pp. 882–893, Nov. 2009, doi: 10.1007/s12045-009-0084-7.

[12] Raza, K., Kumar, P., Ratan, S., Malik, R., & Arora, S. (2014). Polymorphism : The Phenomenon Affecting the Performance of Drugs.

[13] Handa M, Almalki WH, Shukla R, Afzal O, Altamimi ASA, Beg S, Rahman M. Active pharmaceutical ingredients (APIs) in ionic liquids: An effective approach for API physiochemical parameter optimization. Drug Discov Today. 2022 Sep;27(9):2415-2424. doi: 10.1016/j.drudis.2022.06.003

[14] J. A. G. Morais and M. D. R. Lobato, "The new european medicines agency guideline on the investigation of bioequivalence," in *Basic and Clinical Pharmacology and Toxicology*, Mar. 2010, pp. 221–225. doi: 10.1111/j.1742-7843.2009.00518.x.

[15] D. B. Kell, "The transporter-mediated cellular uptake of pharmaceutical drugs is based on their metabolite-likeness and not on their bulk biophysical properties: Towards a systems pharmacology," *Perspect Sci (Neth)*, vol. 6, pp. 66–83, Dec. 2015, doi: 10.1016/j.pisc.2015.06.004.

[16] O. D. Bakulina, M. Y. Ivanov, D. V. Alimov, S. A. Prikhod'ko, N. Y. Adonin, and M. V. Fedin, "Active Pharmaceutical Ingredient-Ionic Liquids (API-ILs): Nanostructure of the Glassy State Studied by Electron Paramagnetic Resonance Spectroscopy," *Molecules*, vol. 27, no. 16, Aug. 2022, doi: 10.3390/molecules27165117.

[17] I. M. Marrucho, L. C. Branco, and L. P. N. Rebelo, "Ionic liquids in pharmaceutical applications," *Annual Review of Chemical and Biomolecular Engineering*, vol. 5. Annual Reviews Inc., pp. 527–546, 2014. doi: 10.1146/annurev-chembioeng-060713-040024.

[18] D. Gupta, D. Bhatia, V. Dave, V. Sutariya, and S. V. Gupta, "Salts of therapeutic agents: Chemical, physicochemical, and biological considerations," *Molecules*, vol. 23, no. 7. MDPI AG, 2018. doi: 10.3390/molecules23071719.

[19] A. F. M. Cláudio, M. C. Neves, K. Shimizu, J. N. Canongia Lopes, M. G. Freire, and J. A. P. Coutinho, "The magic of aqueous solutions of ionic liquids: Ionic liquids as a powerful class of catanionic hydrotropes," *Green Chemistry*, vol. 17, no. 7, pp. 3948–3963, Jul. 2015, doi: 10.1039/c5gc00712g.

[20] S. N. Pedro, C. S. R. Freire, A. J. D. Silvestre, and M. G. Freire, "The role of ionic liquids in the pharmaceutical field: An overview of relevant applications," *International Journal of Molecular Sciences*, vol. 21, no. 21. MDPI AG, pp. 1–50, Nov. 01, 2020. doi: 10.3390/ijms21218298.

[21] F. S. Buarque, G. V. Gautério, M. A. Z. Coelho, A. C. Lemes, and B. D. Ribeiro, "Aqueous Two-Phase Systems Based on Ionic Liquids and Deep Eutectic Solvents as a Tool for the Recovery of Non-Protein Bioactive Compounds—A Review," *Processes*, vol. 11, no. 1. MDPI, Jan. 01, 2023. doi: 10.3390/pr11010031.

[22] Bica K, Rodríguez H, Gurau G, Cojocaru OA, Riisager A, Fehrmann R, Rogers RD. Pharmaceutically active ionic liquids with solids handling, enhanced thermal stability, and fast release. Chem Commun (Camb). 2012 Jun 4;48(44):5422-4. doi: 10.1039/c2cc30959a.

[23] L. Viau, C. Tourné-Péteilh, J. M. Devoisselle, and A. Vioux, "Ionogels as drug delivery system: One-step sol-gel synthesis using imidazolium ibuprofenate ionic liquid," *Chemical Communications*, vol. 46, no. 2, pp. 228–230, 2010, doi: 10.1039/b913879j.

[24] N. R. Jadhav, S. P. Bhosale, S. S. Bhosale, S. D. Mali, P. B. Toraskar, and T. S. Kadam, "Ionic liquids: Formulation avenues, drug delivery and therapeutic updates," *Journal of Drug Delivery Science and Technology*, vol. 65. Editions de Sante, Oct. 01, 2021. doi: 10.1016/j.jddst.2021.102694.

[25] S. N. Pedro, C. S. R. Freire, A. J. D. Silvestre, and M. G. Freire, "Ionic Liquids in Drug Delivery," *Encyclopedia*, vol. 1, no. 2, pp. 324–339, Apr. 2021, doi: 10.3390/encyclopedia1020027.

[26] C. Liu, B. Chen, W. Shi, W. Huang, and H. Qian, "Ionic Liquids for Enhanced Drug Delivery: Recent Progress and Prevailing Challenges," *Molecular Pharmaceutics*, vol. 19, no. 4. American Chemical Society, pp. 1033–1046, Apr. 04, 2022. doi: 10.1021/acs.molpharmaceut.1c00960.

[27] A. Balk, J. Wiest, T. Widmer, B. Galli, U. Holzgrabe, and L. Meinel, "Transformation of acidic poorly water soluble drugs into ionic liquids," *European Journal of Pharmaceutics and Biopharmaceutics*, vol. 94, pp. 73–82, Aug. 2015, doi: 10.1016/j.ejpb.2015.04.034.

[28] M. M. Santos *et al.*, "Ionic Liquids and Salts from Ibuprofen as Promising Innovative Formulations of an Old Drug," *ChemMedChem*, vol. 14, no. 9, pp. 907–911, May 2019, doi: 10.1002/cmdc.201900040.

[29] T. E. Sintra, D. O. Abranches, J. Benfica, B. P. Soares, S. P. M. Ventura, and J. A. P. Coutinho, "Cholinium-based ionic liquids as bioinspired hydrotropes to tackle solubility challenges in drug formulation," *European Journal of Pharmaceutics and Biopharmaceutics*, vol. 164, pp. 86–92, Jul. 2021, doi: 10.1016/j.ejpb.2021.04.013.

[30] F. Endres, "Physical chemistry of ionic liquids," *Physical Chemistry Chemical Physics*, vol. 12, no. 8, pp. 1648–1648, Feb. 2010, doi: 10.1039/c001176m.

[31] G. Lafforgue *et al.*, "Oral absorption of ampicillin: Role of paracellular route vs. PepT1 transporter," *Fundam Clin Pharmacol*, vol. 22, no. 2, pp. 189–201, Apr. 2008, doi: 10.1111/j.1472-8206.2008.00572.x.

[32] Branco, L. A. A. F. C., Marrucho, I. M., Araújo, J. M. M., Rebelo, L. P., Nunes da Ponte, M., Prudêncio, C., & Petrovski, Z. (2012). Development of novel ionic liquids based on ampicillin. MedChemComm, 3(4), 494-497. https://doi.org/10.1039/c2md00269h

[33] Florindo C, Araújo JM, Alves F, Matos C, Ferraz R, Prudêncio C, Noronha JP, Petrovski Ž, Branco L, Rebelo LP, Marrucho IM. Evaluation of solubility and partition properties of ampicillin-based ionic liquids. Int J Pharm. 2013 Nov 18;456(2):553-9. doi: 10.1016/j.ijpharm.2013.08.010.

[34] Hough, W.L., Śmiglak, M., Rodríguez, H., Swatloski, R.P., Spear, S.K., Daly, D.T., Pernak, J., Grisel, J.E., Carliss, R., Soutullo, M.D., Davis, J.H., & Rogers, R.D. (2007). The third evolution of ionic liquids: active pharmaceutical ingredients. New Journal of Chemistry, 31, 1429-1436.

[35] Rogers R. D., Bica K., Rodríguez H; Ionic Liquid Technology: A Potential New Platform for the Pharmaceutical Industry 2008; Tropical Journal of Pharmaceutical Research, September 7 (3): 1011-1012

[36] B. D. Anderson*' And and R. A. Conradi, "Predictive Relationships in the Water Solubility of Salts of a Nonsteroidal Anti-inflammatory Drug."

[37] R. Ferraz, L. C. Branco, C. Prudêncio, J. P. Noronha, and Ž. Petrovski, "Ionic liquids as active pharmaceutical ingredients," *ChemMedChem*, vol. 6, no. 6, pp. 975–985, Jun. 2011, doi: 10.1002/cmdc.201100082.

[38] V. D. Gholap, A. D. Savkare, P. M. Kukkar, and M. R. Bhavsar, "BIODEGRADABLE STARCH FOAMS AS A DRUG CARRIER," *Indo American Journal of Pharmaceutical Research*, vol. 2017, no. 03, p. 7, 2017, [Online]. Available: www.iajpr.comwww.iajpr.com

[39] C. A. García-González *et al.*, "An opinion paper on aerogels for biomedical and environmental applications," *Molecules*, vol. 24, no. 9. MDPI AG, 2019. doi: 10.3390/molecules24091815.

[40] A. Soleimani Dorcheh and M. H. Abbasi, "Silica aerogel; synthesis, properties and characterization," *Journal of Materials Processing Technology*, vol. 199, no. 1. pp. 10–26, Apr. 01, 2008. doi: 10.1016/j.jmatprotec.2007.10.060.

[41] A. B. Paninho *et al.*, "A bio-based alginate aerogel as an ionic liquid support for the efficient synthesis of cyclic carbonates from co2 and epoxides," *Catalysts*, vol. 11, no. 8, Aug. 2021, doi: 10.3390/catal11080872.

[42] G. F. Brito, P. Agrawal, E. M. Araújo, and T. J. A. Mélo, "Biopolímeros, Polímeros Biodegradáveis e Polímeros Verdes," no. 2, pp. 127–139, 2011, [Online]. Available: www.braskem.com.br

[43] J. W. Y. Liew, K. S. Loh, A. Ahmad, K. L. Lim, and W. R. Wan Daud, "Synthesis and characterization of modified κ-carrageenan for enhanced proton conductivity as polymer electrolyte membrane," *PLoS One*, vol. 12, no. 9, Sep. 2017, doi: 10.1371/journal.pone.0185313.

[44] W. Ahmad Kamil Mahmood, M. Mizanur Rahman Khan, and T. Cheng Yee, "Effects of Reaction Temperature on the Synthesis and Thermal Properties of Carrageenan Ester," 2014.

[45] C. Hiremath and G. Heggannavar, "Biopolymers in Drug Delivery Applications." [Online]. Available: https://www.researchgate.net/publication/272817366

[46] T. K. Giri, S. Pure, and D. K. Tripathi, "Synthesis of graft copolymers of acrylamide for locust bean gum using microwave energy: Swelling behavior, flocculation characteristics and acute toxicity study," *Polimeros*, vol. 25, no. 2, pp. 168–174, Mar. 2015, doi: 10.1590/0104-1428.1717.

[47] R. Couto Alves and M. Gabriela Novy Quadri, "UNIVERSIDADE FEDERAL DE SANTA CATARINA DEPARTAMENTO DE ENGENHARIA QUÍMICA E ENGENHARIA DE ALIMENTOS PROGRAMA DE PÓS-GRADUAÇÃO EM ENGENHARIA QUÍMICA," 2013.

[48] J. T. Martins, M. A. Cerqueira, A. I. Bourbon, A. C. Pinheiro, B. W. S. Souza, and A. A. Vicente, "Synergistic effects between κ-carrageenan and locust bean gum on physicochemical properties of edible films made thereof," *Food Hydrocoll*, vol. 29, no. 2, pp. 280–289, Dec. 2012, doi: 10.1016/j.foodhyd.2012.03.004.

[49] P. A. Dakia, B. Wathelet, and M. Paquot, "Isolation and chemical evaluation of carob (Ceratonia siliqua L.) seed germ," *Food Chem*, vol. 102, no. 4, pp. 1368–1374, 2007, doi: 10.1016/j.foodchem.2006.05.059.

[50] P. B. Fernandes, M. P. Gonçalves, and J. L. Doublier, "Phase diagrams in kappa-carrageenan/locust bean gum systems," *Top Catal*, vol. 5, no. 1–2, pp. 71–73, 1991, doi: 10.1016/S0268-005X(09)80289-0.

[51] J. T. Martins, M. A. Cerqueira, A. I. Bourbon, A. C. Pinheiro, B. W. S. Souza, and A. A. Vicente, "Synergistic effects between κ-carrageenan and locust bean gum on physicochemical properties of edible films made thereof," *Food Hydrocoll*, vol. 29, no. 2, pp. 280–289, Dec. 2012, doi: 10.1016/j.foodhyd.2012.03.004.

[52] S. Barak and D. Mudgil, "Locust bean gum: Processing, properties and food applications-A review," *International Journal of Biological Macromolecules*, vol. 66. Elsevier B.V., pp. 74–80, 2014. doi: 10.1016/j.ijbiomac.2014.02.017.

[53] T. Mehling, I. Smirnova, U. Guenther, and R. H. H. Neubert, "Polysaccharide-based aerogels as drug carriers," *J Non Cryst Solids*, vol. 355, no. 50–51, pp. 2472–2479, Dec. 2009, doi: 10.1016/j.jnoncrysol.2009.08.038.

[54] S. Zhao, W. J. Malfait, N. Guerrero-Alburquerque, M. M. Koebel, and G. Nyström, "Biopolymer Aerogels and Foams: Chemistry, Properties, and Applications," *Angewandte*

Chemie - International Edition, vol. 57, no. 26. Wiley-VCH Verlag, pp. 7580–7608, Jun. 25, 2018. doi: 10.1002/anie.201709014.

[55] G. Tkalec, Ž. Knez, and Z. Novak, "Fast production of high-methoxyl pectin aerogels for enhancing the bioavailability of low-soluble drugs," *Journal of Supercritical Fluids*, vol. 106, pp. 16–22, Nov. 2015, doi: 10.1016/j.supflu.2015.06.009.

[56] Z. Ulker and C. Erkey, "An emerging platform for drug delivery: Aerogel based systems," *Journal of Controlled Release*, vol. 177, no. 1. Elsevier B.V., pp. 51–63, Mar. 10, 2014. doi: 10.1016/j.jconrel.2013.12.033.

[57] R. Gul, N. Ahmed, K. U. Shah, G. M. Khan, and Asim.ur.Rehman, "Functionalised nanostructures for transdermal delivery of drug cargos," *Journal of Drug Targeting*, vol. 26, no. 2. Taylor and Francis Ltd, pp. 110–122, Feb. 07, 2018. doi: 10.1080/1061186X.2017.1374388.

[58] M. S. Hosseini, I. Amjadi, M. Mohajeri, M. Zubair Iqbal, A. Wu, and M. Mozafari, "Functional polymers: an introduction in the context of biomedical engineering," in *Advanced Functional Polymers for Biomedical Applications*, Elsevier, 2019, pp. 1–20. doi: 10.1016/B978-0-12-816349-8.00001-1.

[59] Kujawa, J.; Rynkowska, E.; Fatyeyeva, K.; Knozowska, K.; Wolan, A.; Dzieszkowski, K.; Li, G.; Kujawski, W. Preparation and Characterization of Cellulose Acetate Propionate Films Functionalized with Reactive Ionic Liquids. Polymers 2019, 11, 1217. https://doi.org/10.3390/polym11071217

[60] B. Chaurasiya and Y. Y. Zhao, "Dry powder for pulmonary delivery: A comprehensive review," *Pharmaceutics*, vol. 13, no. 1. MDPI AG, pp. 1–28, Jan. 01, 2021. doi: 10.3390/pharmaceutics13010031.

[61] P. C. L. Kwok and H. K. Chan, "Pulmonary drug delivery," *Therapeutic Delivery*, vol. 4, no. 8. pp. 877–878, Aug. 2013. doi: 10.4155/tde.13.89.

[62] M. P. Patel, R. R. Patel, and J. K. Patel, "Chitosan Mediated Targeted Drug Delivery System: A Review," 2010. [Online]. Available: www.cspsCanada.org

[63] T. Sou, L. Orlando, M. P. McIntosh, L. M. Kaminskas, and D. A. V. Morton, "Investigating the interactions of amino acid components on a mannitol-based spray-dried powder formulation for pulmonary delivery: A design of experiment approach," *Int J Pharm*, vol. 421, no. 2, pp. 220–229, Dec. 2011, doi: 10.1016/j.ijpharm.2011.09.018.

[64] A. H. L. Chow, H. H. Y. Tong, P. Chattopadhyay, and B. Y. Shekunov, "Particle engineering for pulmonary drug delivery," *Pharmaceutical Research*, vol. 24, no. 3. pp. 411–437, Mar. 2007. doi: 10.1007/s11095-006-9174-3.

[65] B. Díaz-Reinoso, A. Moure, H. Domínguez, and J. C. Parajó, "Supercritical CO2 extraction and purification of compounds with antioxidant activity," *Journal of Agricultural and Food Chemistry*, vol. 54, no. 7. pp. 2441–2469, Apr. 05, 2006. doi: 10.1021/jf052858j.

[66] C. Costa, T. Casimiro, and A. Aguiar-Ricardo, "Optimization of Supercritical CO2-Assisted Atomization: Phase Behavior and Design of Experiments," *Journal of Chemical and Engineering Data*, vol. 63, no. 4. American Chemical Society, pp. 885–896, Apr. 12, 2018. doi: 10.1021/acs.jced.7b00820.

[67] D. Zillen, M. Beugeling, W. L. J. Hinrichs, H. W. Frijlink, and F. Grasmeijer, "Natural and bioinspired excipients for dry powder inhalation formulations," *Current Opinion in Colloid and Interface Science*, vol. 56. Elsevier Ltd, Dec. 01, 2021. doi: 10.1016/j.cocis.2021.101497.

[68] L. C. Branco, J. N. Rosa, J. J. Moura Ramos, and C. A. M. Afonso, "Preparation and characterization of new room temperature ionic liquids," *Chemistry - A European Journal*, vol. 8, no. 16, pp. 3671–3677, Aug. 2002, doi: 10.1002/1521-3765(20020816)8:16<3671::AID-CHEM3671>3.0.CO;2-9.

[69] A. R. C. Duarte, A. S. D. Ferreira, S. Barreiros, E. Cabrita, R. L. Reis, and A. Paiva, "A comparison between pure active pharmaceutical ingredients and therapeutic deep eutectic solvents: Solubility and permeability studies," *European Journal of Pharmaceutics and Biopharmaceutics*, vol. 114, pp. 296–304, May 2017, doi: 10.1016/j.ejpb.2017.02.003.

[70] B. L. Gadilohar and G. S. Shankarling, "Choline based ionic liquids and their applications in organic transformation," *Journal of Molecular Liquids*, vol. 227. Elsevier B.V., pp. 234–261, Feb. 01, 2017. doi: 10.1016/j.molliq.2016.11.136.

[71] Ledeți I, Ledeți A, Vlase G, Vlase T, Matusz P, Bercean V, Şuta LM, Piciu D. Thermal stability of synthetic thyroid hormone l-thyroxine and l-thyroxine sodium salt hydrate both pure and in pharmaceutical formulations. J Pharm Biomed Anal. 2016 Jun 5;125:33-40. doi: 10.1016/j.jpba.2016.03.026.

[72] Ledeți, I.; Romanescu, M.; Cîrcioban, D.; Ledeți, A.; Vlase, G.; Vlase, T.; Suciu, O.; Murariu, M.; Olariu, S.; Matusz, P.; et al. Stability and Compatibility Studies of Levothyroxine Sodium in Solid Binary Systems—Instrumental Screening. Pharmaceutics 2020, 12, 58. https://doi.org/10.3390/pharmaceutics12010058

[73] J. W. Collier, R. B. Shah, A. Gupta, V. Sayeed, M. J. Habib, and M. A. Khan, "Influence of formulation and processing factors on stability of levothyroxine sodium pentahydrate," *AAPS PharmSciTech*, vol. 11, no. 2, pp. 818–825, Jun. 2010, doi: 10.1208/s12249-010-9434-8.

[74] S. Mondal and G. Mugesh, "Structure Elucidation and Characterization of Different Thyroxine Polymorphs," *Angewandte Chemie*, vol. 127, no. 37, pp. 10983–10987, Sep. 2015, doi: 10.1002/ange.201505281.

[75] M. Arici, E. Oztas, F. Yanar, N. Aksakal, B. Ozcinar, and G. Ozhan, "Association between genetic polymorphism and levothyroxine bioavailability in hypothyroid patients," *Endocr J*, vol. 65, no. 3, pp. 317–323, 2018, doi: 10.1507/endocrj.EJ17-0162.

[76] D. Braga, L. Casali, and F. Grepioni, "The Relevance of Crystal Forms in the Pharmaceutical Field: Sword of Damocles or Innovation Tools?," *International Journal of Molecular Sciences*, vol. 23, no. 16. MDPI, Aug. 01, 2022. doi: 10.3390/ijms23169013.

[77] K. T. Savjani, A. K. Gajjar, and J. K. Savjani, "Drug Solubility: Importance and Enhancement Techniques," *ISRN Pharm*, vol. 2012, pp. 1–10, Jul. 2012, doi: 10.5402/2012/195727.

[78] N. Barton, "Thyroid Preparations," in *Encyclopedia of Toxicology: Third Edition*, Elsevier, 2014, pp. 570–572. doi: 10.1016/B978-0-12-386454-3.00795-8.

[79] "Evert, Henry E. (1960). THE SOLUBILITY OF l-THYROXINE (Na) IN THE PRESENCE OF PHOSPHATE BUFFER AND OF NEUTRAL SALTS. The Journal of Physical Chemistry, 64(4), 478–480.".

[80] M. Robitzer, Audrey Tourette, R. Horga, R. Valentin, Michel Boissière, Nitrogen sorption as a tool for the characterisation of polysaccharide aerogels. Carbohydrate Polymers, 2011, 85 (1), pp.44-53. (10.1016/j.carbpol.2011.01.040)

[81] M. Robitzer, L. David, C. Rochas, F. Di Renzo, and F. Quignard, "Nanostructure of calcium alginate aerogels obtained from multistep solvent exchange route," *Langmuir*, vol. 24, no. 21, pp. 12547–12552, 2008, doi: 10.1021/la802103t.

[82] R. Valentin, K. Molvinger, C. Viton, A. Domard, and F. Quignard, "From hydrocolloids to high specific surface area porous supports for catalysis," *Biomacromolecules*, vol. 6, no. 5, pp. 2785–2792, 2005, doi: 10.1021/bm050264j.

[83] F. Quignard, F. Di Renzo, and E. Guibal, "From Natural Polysaccharides to Materials for Catalysis, Adsorption, and Remediation," 2010, pp. 165–197. doi: 10.1007/128_2010_56.

[84] F. Quignard, R. Valentin, and F. Di Renzo, "Aerogel materials from marine polysaccharides," *New Journal of Chemistry*, vol. 32, no. 8, p. 1300, 2008, doi: 10.1039/b808218a.

[85] C. Tsioptsias, C. Michailof, G. Stauropoulos, and C. Panayiotou, "Chitin and carbon aerogels from chitin alcogels," *Carbohydr Polym*, vol. 76, no. 4, pp. 535–540, 2009, doi: 10.1016/j.carbpol.2008.11.018.

[86] X. Chang, D. Chen, and X. Jiap, "Chitosan-based aerogels with high adsorption performance," *Journal of Physical Chemistry B*, vol. 112, no. 26, pp. 7721–7725, 2008, doi: 10.1021/jp8011359.

[87] M. G. Ventura, A. I. Paninho, A. V. M. Nunes, I. M. Fonseca, and L. C. Branco, "Biocompatible locust bean gum mesoporous matrices prepared by ionic liquids and a scCO $_2$ sustainable system," *RSC Adv.*, vol. 5, no. 130, pp. 107700–107706, 2015, doi: 10.1039/C5RA17314K.

[88] C. Costa *et al.*, "Inhalable hydrophilic molecule-loaded liposomal dry powder formulations using supercritical CO2 – assisted spray-drying," *Journal of CO2 Utilization*, vol. 53, Nov. 2021, doi: 10.1016/j.jcou.2021.101709.

[89] Bernardes. A (2022) New Fight Against Tuberculosis using Pharmaceutical Ionic Liquids, [Master's degree, Nova School of Science and Technology FCT-NOVA]. FCT-NOVA Research

[90] K. Berkenfeld, J. T. McConville, and A. Lamprecht, "Inhalable dry powders of rifampicin highlighting potential and drawbacks in formulation development for experimental tuberculosis aerosol therapy," *Expert Opinion on Drug Delivery*, vol. 17, no. 3. Taylor and Francis Ltd, pp. 305–322, Mar. 03, 2020. doi: 10.1080/17425247.2020.1720644.

[91] Ledeţi I, Romanescu M, Cîrcioban D, Ledeţi A, Vlase G, Vlase T, Suciu O, Murariu M, Olariu S, Matusz P, Buda V, Piciu D. Stability and Compatibility Studies of Levothyroxine Sodium in Solid Binary Systems-Instrumental Screening. Pharmaceutics. 2020 Jan 10;12(1):58. doi: 10.3390/pharmaceutics12010058.

[92] Costa P, Sousa Lobo JM. Modeling and comparison of dissolution profiles. Eur J Pharm Sci. 2001 May;13(2):123-33. doi: 10.1016/s0928-0987(01)00095-1.

[93] Singhvi, G., Mahaveer S., In vitro Drug Release Characterization Models (2011), International Journal of Pharmaceutical Studies and Research. 2. 77-84.

[94] Philip L. Ritger, Nikolaos A. Peppas, 1987, Transport of penetrants in the macromolecular structure of coals: Models for analysis of dynamic penetrant transport, Fuel, V. 66, Issue 6,815-826, doi: 10.1016/0016-2361(87)90130-X.

[95] B. N. Estevinho, F. Rocha, L. Santos, and A. Alves, "Microencapsulation with chitosan by spray drying for industry applications - A review," *Trends in Food Science and Technology*, vol. 31, no. 2. pp. 138–155, Jun. 2013. doi: 10.1016/j.tifs.2013.04.001.

[96] P. L. Ritger and N. A. Peppas, "A SIMPLE EQUATION FOR DESCRIPTION OF SOLUTE RELEASE II. FICKIAN AND ANOMALOUS RELEASE FROM SWELLABLE DEVICES," Elsevier Science Publishers B.V, 1987.

[97] P. J. Cox, K. A. Khan, D. L. Munday, and J. Sujja-Areevath, "Development and evaluation of a multiple-unit oral sustained release dosage form for S(+)-ibuprofen: preparation and release kinetics," 1999. [Online]. Available: www.elsevier.com/locate/ijpharm

[98] Samineni R, Chimakurthy J, Konidala S. Emerging Role of Biopharmaceutical Classification and Biopharmaceutical Drug Disposition System in Dosage form Development:

A Systematic Review. Turk J Pharm Sci. 2022 Dec 21;19(6):706-713. doi: 10.4274/tjps.galenos.2021.73554.

[99] K. Nahar *et al.*, "In vitro, in vivo and ex vivo models for studying particle deposition and drug absorption of inhaled pharmaceuticals," *European Journal of Pharmaceutical Sciences*, vol. 49, no. 5. Elsevier B.V., pp. 805–818, 2013. doi: 10.1016/j.ejps.2013.06.004.

A

APPENDIX

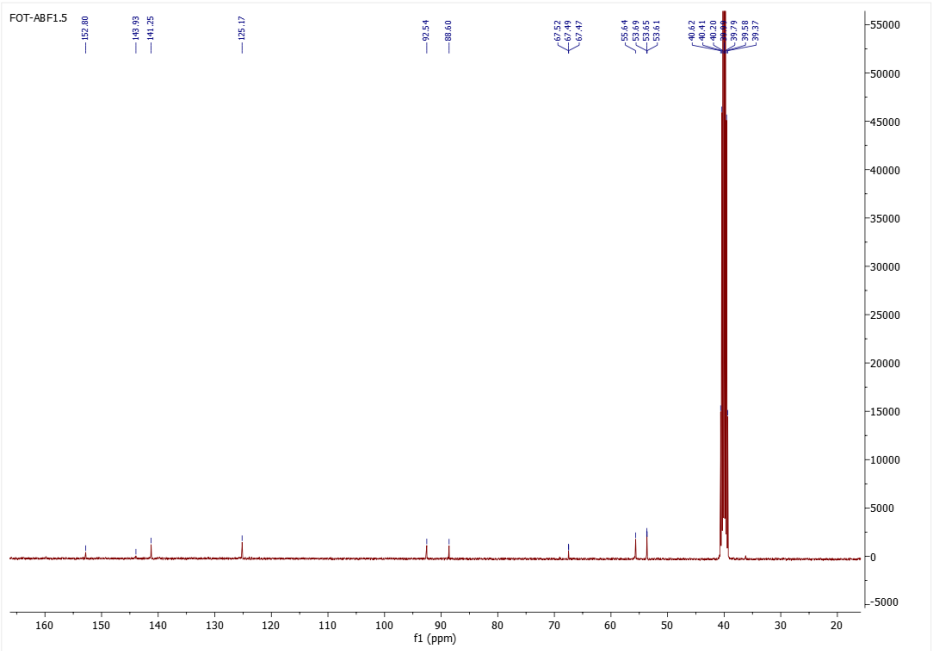

Appendix 1 - ^{13}C NMR [Ch][T4]

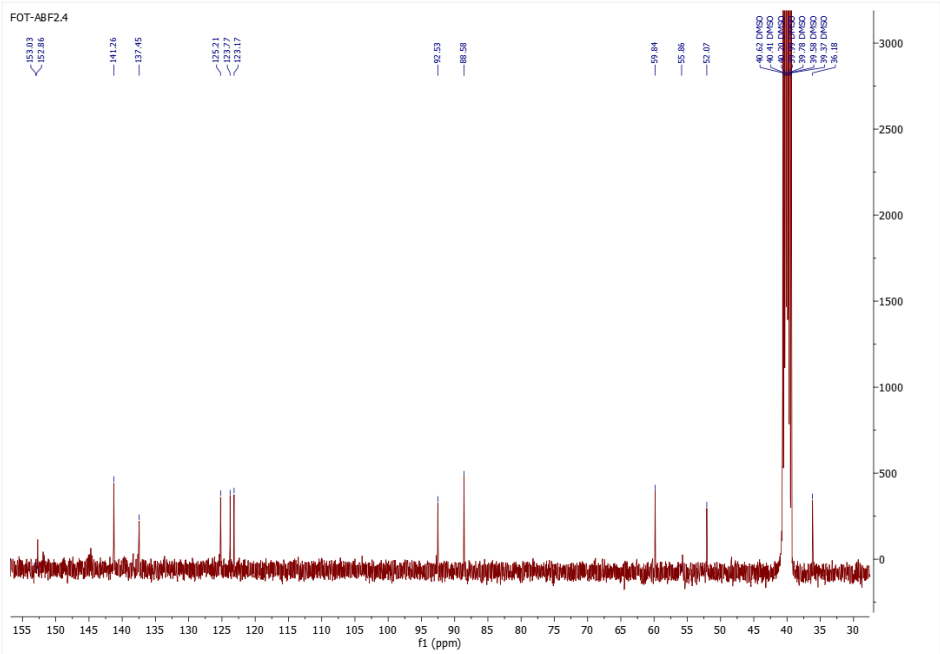

Appendix 2 - ^{13}C NMR [C_2OHMIM][T4]

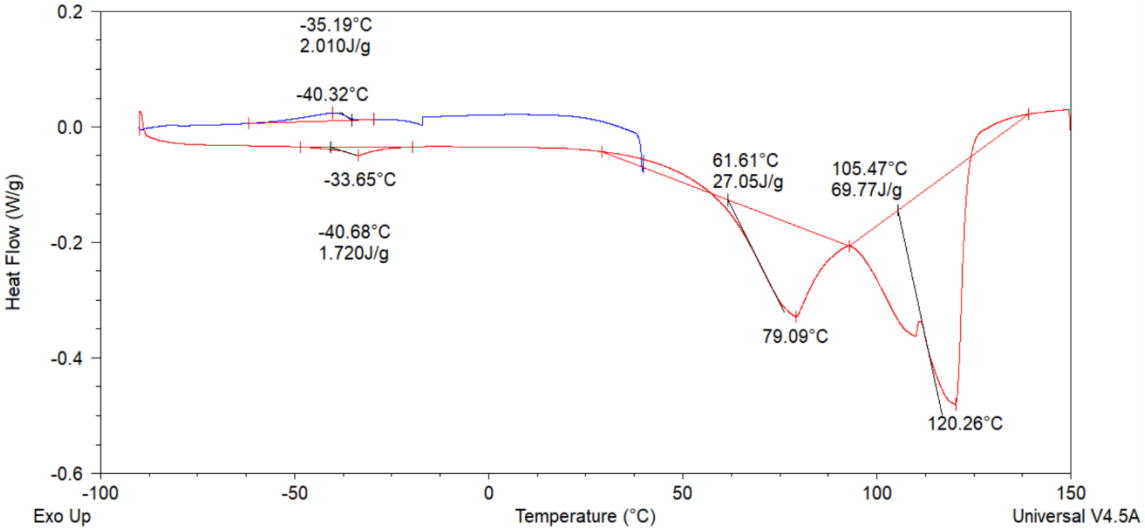

Appendix 3 - Thermogram of neat levothyroxine with the corresponding temperature phase transitions and enthalpies

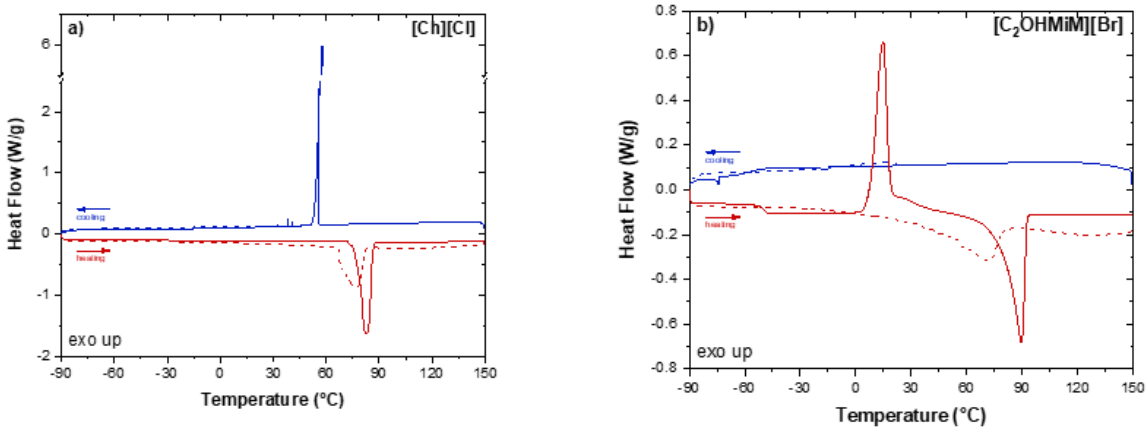

Appendix 4 - Thermograms for the starting ionic liquids: a) [Ch][Cl] and b) [C_2OHMiM][Br]. Dashed lines represent the first heating and cooling runs, whereas the solid lines correspond to the second heating and cooling runs

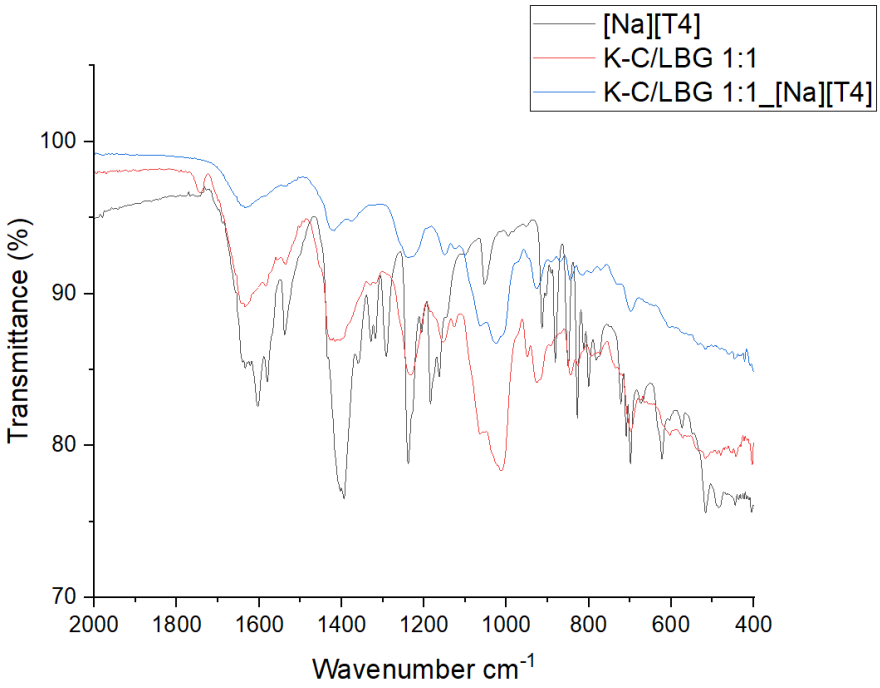

Appendix 5 - FTIR spectra of K-C/LBG 1:1 impregnated with [Na][T4]

	Element (%)			
Sample	N	C	H	S
K-C/LBG	0.44	32.32	5.57	2.61
K-C/LBG 1:1	1.08	34.56	5.44	2.92
K-C/LBG 1:6	3.49	30.34	4.84	1.84

Appendix 6 - Elemental analysis of biopolymers functionalized and non-functionalized with [EO-MIM][Br] (K-C/LBG; 1:1; 1:6)

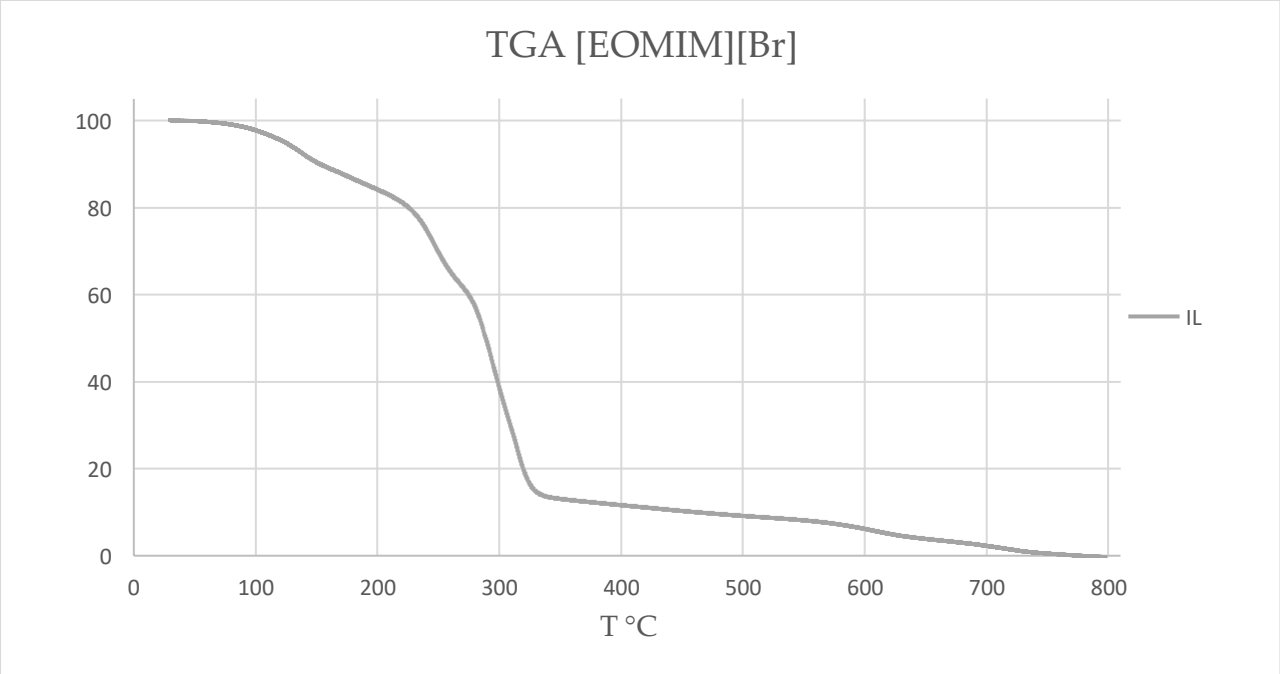

Appendix 7 - TGA of IL [EOMIM][Br]

Weight (mg)				
[Na][T4]	**Before loading [Na][T4]**	**After loading [Na][T4]**	**Mass [Na][T4] (mg)**	**q (mg/g)**
K-C/LBG 0_0	4.8	11.5	6.7	1200.4
K-C/LBG 1_1	5.2	13.7	8.5	1405.8
K-C/LBG 1_6	5.3	11.2	5.9	957.4
[Ch][T4] (89,3% T4)	**Before loading**	**After loading**	**Mass [Na][T4] (mg)**	**q (mg/g)**
K-C/LBG 0_0	5.2	14.3	9.1	1505.0
K-C/LBG 1_1	3.8	7.2	3.4	769.5
K-C/LBG 1_6	5.6	8.2	2.6	399.3
[C_2OHMIM][T4] (87,2% T4)	**Before loading**	**After loading**	**Mass [Na][T4] (mg)**	**q (mg/g)**
K-C/LBG 0_0	4.7	10.4	5.7	1043.0
K-C/LBG 1_1	4.8	9.9	5.1	913.8
K-C/LBG 1_6	3.3	5.9	2.6	677.6

Appendix 8 - Gravimetric analysis weight variation before and after [Na][T4], [Ch][T4] and [C_2OHMIM][T4] encapsulation

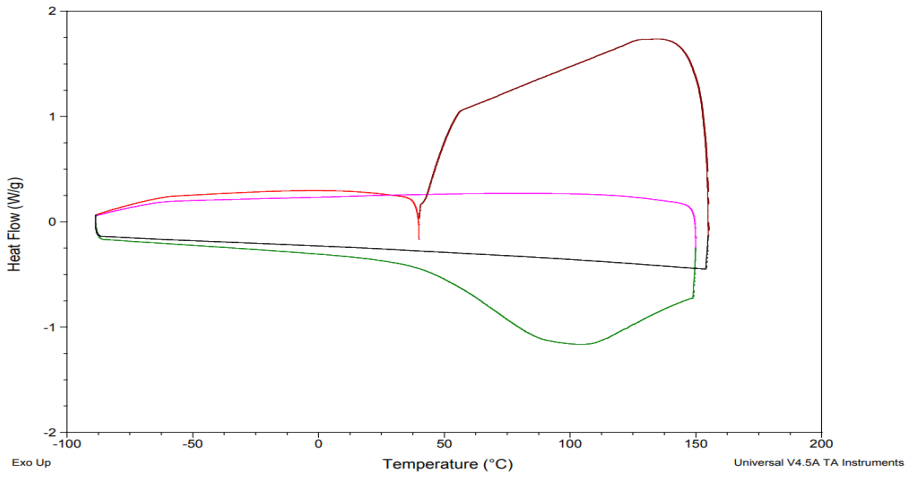

Appendix 9 - DSC of K-C/LBG

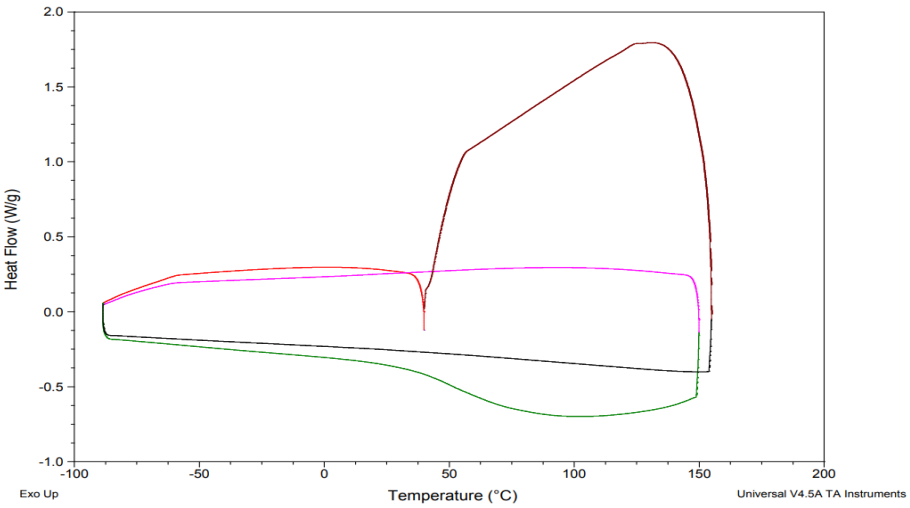

Appendix 10 - DSC of K-C/LBG_[T4]

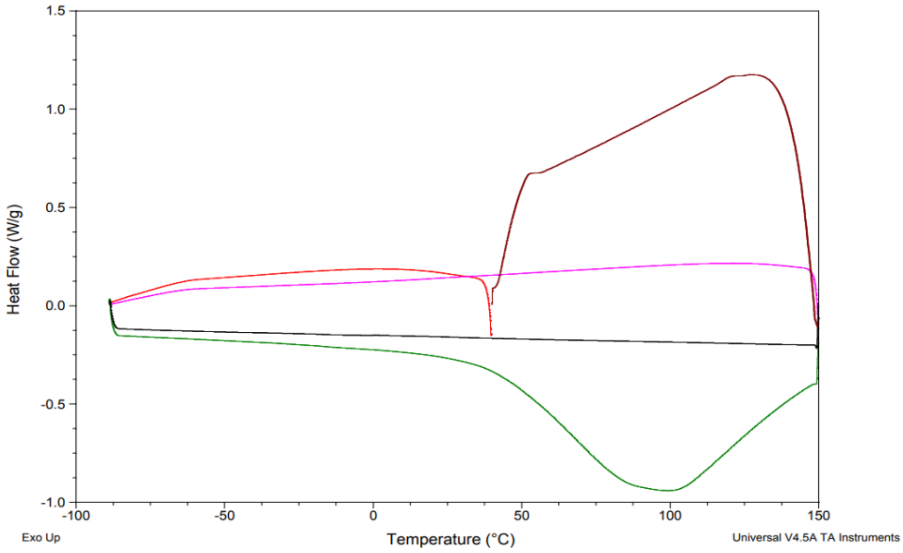

Appendix 11 - DSC of K-C/LBG 1:1

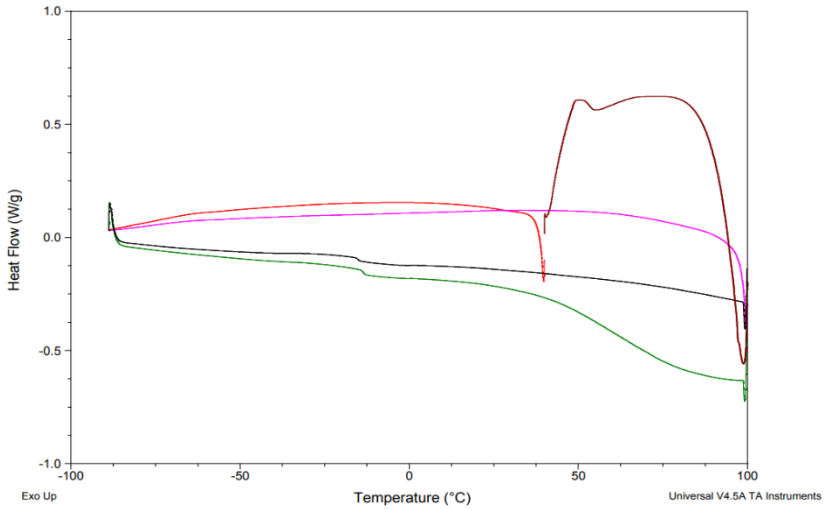

Appendix 12 - DSC of K-C/LBG 1:1_[T4]

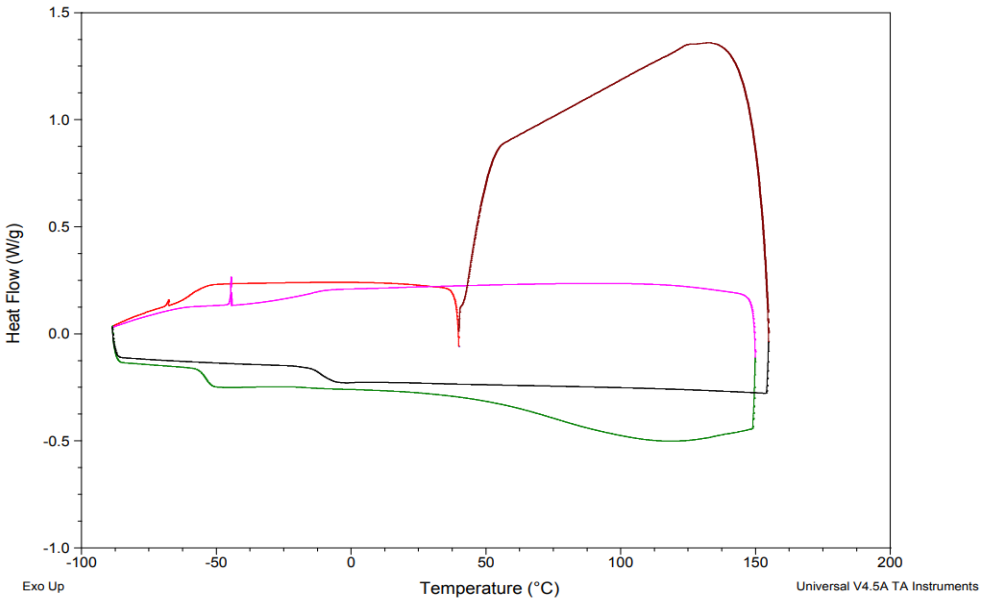

Appendix 13 - DSC of IL [EOMIM[Br]